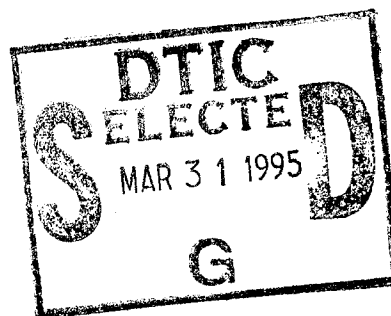


NAVAL POSTGRADUATE SCHOOL MONTEREY, CALIFORNIA



19950329 065



THESIS

**CONTINENTAL AEROSOL EFFECTS ON
STRATOCUMULUS MICROPHYSICS
DURING MAST 1994**

by

Joseph R. Brenner

December, 1994

Thesis Advisor:

Philip A. Durkee

Approved for public release; distribution is unlimited.

REPORT DOCUMENTATION PAGE			Form Approved OMB No. 0704-0188	
Public reporting burden for this collection of information is estimated to average 1 hour per response, including the time for reviewing instruction, searching existing data sources, gathering and maintaining the data needed, and completing and reviewing the collection of information. Send comments regarding this burden estimate or any other aspect of this collection of information, including suggestions for reducing this burden, to Washington Headquarters Services, Directorate for Information Operations and Reports, 1215 Jefferson Davis Highway, Suite 1204, Arlington, VA 22202-4302, and to the Office of Management and Budget, Paperwork Reduction Project (0704-0188) Washington DC 20503.				
1. AGENCY USE ONLY (Leave blank)		2. REPORT DATE December 1994		3. REPORT TYPE AND DATES COVERED Master's Thesis
4. TITLE AND SUBTITLE CONTINENTAL AEROSOL EFFECTS ON STRATOCUMULUS MICROPHYSICS DURING MAST 1994			5. FUNDING NUMBERS	
6. AUTHOR(S) Joseph R. Brenner				
7. PERFORMING ORGANIZATION NAME(S) AND ADDRESS(ES) Naval Postgraduate School Monterey CA 93943-5000			8. PERFORMING ORGANIZATION REPORT NUMBER	
9. SPONSORING/MONITORING AGENCY NAME(S) AND ADDRESS(ES)			10. SPONSORING/MONITORING AGENCY REPORT NUMBER	
11. SUPPLEMENTARY NOTES The views expressed in this thesis are those of the author and do not reflect the official policy or position of the Department of Defense or the U.S. Government.				
12a. DISTRIBUTION/AVAILABILITY STATEMENT Approved for public release; distribution is unlimited.			12b. DISTRIBUTION CODE	
13. ABSTRACT (maximum 200 words) Variations in marine stratocumulus clouds during the MAST (Monterey Area Ship Tracks) Experiment of June 1994 are observed and analyzed through the use of NOAA-9/10/11/12 AVHRR satellite data. The relationship between channel 3 reflectance and cloud microphysical properties is examined through direct observation of pixel brightness and aerosol trajectories based on a pollutant transport and dispersion model. Satellite observations show significant regions of continental influence over the ocean through higher channel 3 reflectance values as a result of the injection of anthropogenic aerosols. Forward and backward aerosol trajectories are used to show correlation of cloud albedo enhanced regions and the probable routes of continental aerosol injection in the marine environment. This technique may prove useful for determining climatic implications of cloud reflectance changes due to the influence of natural and man-made aerosol sources, and a means for predicting enhanced cloudiness in littoral regions.				
14. SUBJECT TERMS anthropogenic aerosol, trajectory, HY-SPLIT, shiptrack, AVHRR			15. NUMBER OF PAGES *69	
			16. PRICE CODE	
17. SECURITY CLASSIFICATION OF REPORT Unclassified	18. SECURITY CLASSIFICATION OF THIS PAGE Unclassified	19. SECURITY CLASSIFICATION OF ABSTRACT Unclassified	20. LIMITATION OF ABSTRACT UL	

Approved for public release; distribution is unlimited.

**CONTINENTAL AEROSOL EFFECTS ON
STRATOCUMULUS MICROPHYSICS
DURING MAST 1994**

by

Joseph R. Brenner
Lieutenant, United States Navy
B.S., U. S. Naval Academy, 1988

Submitted in partial fulfillment
of the requirements for the degree of

Accession For	
NTIS CRA&I	<input checked="" type="checkbox"/>
DTIC TAB	<input type="checkbox"/>
Unannounced	<input type="checkbox"/>
Justification	
By	
Distribution /	
Availability Codes	
Dist	Avail and/or Special
A-1	

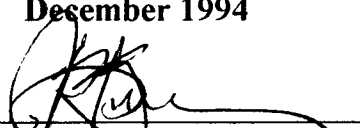
MASTER OF SCIENCE IN METEOROLOGY AND OCEANOGRAPHY

from the

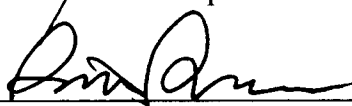
NAVAL POSTGRADUATE SCHOOL

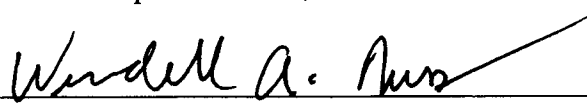
December 1994

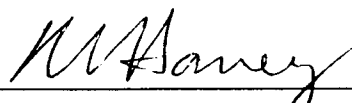
Author:


Joseph R. Brenner

Approved by:


Philip A. Durkee, Thesis Advisor


Wendell A. Nuss, Second Reader


Robert L. Haney, Chairman
Department of Meteorology

ABSTRACT

Variations in marine stratocumulus clouds during the MAST (Monterey Area Ship Tracks) Experiment of June 1994 are observed and analyzed through the use of NOAA-9/10/11/12 AVHRR satellite data. The relationship between channel 3 reflectance and cloud microphysical properties is examined through direct observation of pixel brightness and aerosol trajectories based on a pollutant transport and dispersion model. Satellite observations show significant regions of continental influence over the ocean through higher channel 3 reflectance values as a result of the injection of anthropogenic aerosols. Forward and backward aerosol trajectories are used to show correlation of cloud albedo enhanced regions and the probable routes of continental aerosol injection in the marine environment. This technique may prove useful for determining climatic implications of cloud reflectance changes due to the influence of natural and man-made aerosol sources, and a means for predicting enhanced cloudiness in littoral regions.

TABLE OF CONTENTS

I. INTRODUCTION	1
A. BACKGROUND AND MOTIVATION	1
1. Aerosol Effects On Electro-Optical Devices	2
2. Aerosol Effects On Climate	4
B. MONTEREY AREA SHIPTRACK (MAST) EXPERIMENT	5
C. CLIMATOLOGY OF STRATUS	7
II. THEORY	9
A. AEROSOLS	9
1. Anthropogenic Aerosol	9
B. CLOUD PHYSICS	10
1. Cloud Condensation Nuclei (CCN)	10
C. RADIATIVE PROPERTIES	13
1. Reflectivity	13
2. Low-Cloud Reflectance at AVHRR Channel 3	14
3. Anisotropy	14
III. METHOD OF DATA ANALYSIS	15
A. OVERVIEW	15
B. SATELLITE RETRIEVAL TECHNIQUE	16
C. HY-SPLIT MODEL	16
IV. CASE STUDY RESULTS AND EVALUATION	21
A. CLASSIFICATION OF TRAJECTORY TYPE	21
B. CASE 1 (11 June):	22
1. Synoptic Summary	22

2. Trajectory Synopsis	22
C. CASE 2 (13 June):	25
1. Synoptic Summary	25
2. Trajectory Synopsis	27
3. Additional Comments	27
D. CASE 3 (21 June):	31
1. Synoptic Summary	31
2. Trajectory Synopsis	31
3. Additional Comments	34
E. CASE 4 (29 June):	34
1. Synoptic Summary	34
2. Trajectory Synopsis	34
F. CASE 5 (June 30):	36
1. Synoptic Summary	36
2. Trajectory Synopsis	36
3. Additional Comments	36
G. SATELLITE IMAGE COMPOSITES	39
1. Comparative Streamline Analysis For 13 June and 21 June	39
H. RESULTS	43
V. CONCLUSIONS AND RECOMMENDATIONS	47
A. CONCLUSIONS	47
B. RECOMMENDATIONS	48
APPENDIX	49
LIST OF REFERENCES	56
INITIAL DISTRIBUTION LIST	59

ACKNOWLEDGMENTS

The author is indebted to Professor Philip A. Durkee of the Department of Meteorology at the Naval Postgraduate School. This project would not have been possible without his guidance and support. A special thanks to Professor Wendell A. Nuss and Chairman Robert L. Haney for their careful review of this manuscript. Mr. Chuck Skupniewicz and Kurt E. Neilson have been uniformly supportive and generously helpful in the areas of TereScan and Unix, and the various other programming skills and tasks required for running NOAA's HY-SPLIT Model. This work could not have been completed without their assistance. Thank you to Melinda S. Peng for partitioning space on her IBM RS-6000. Recognition of NOAA's Air Resources Laboratory who allowed the use of the Roland R. Draxler's HY-SPLIT Model and especially Barbara J. B. Stunder whose continued help with a steady stream of data and literature was greatly appreciated. Finally, a dept of gratitude to my family whose undaunted love and support gave me the extra push required to complete this task. The author is solely responsible for any errors or omissions in this text.

I. INTRODUCTION

A. BACKGROUND AND MOTIVATION

Man has affected profound influence on the earth's atmosphere in the last century. The majority of the focus on this climactic response has been in the area of the so-called greenhouse gasses like carbon dioxide. Yet, it is commonly recognized that water, in the form of clouds, is the key factor in atmospheric radiative processes. Cloud microphysics that effect reflectance are dependent upon cloud droplet size, thickness, and liquid water content in conjunction with cloud condensation nuclei (CCN). Aerosol then, form the link between these 'cloud seeds' or CCN and the climactic response due to modifications of cloud parameters. The goal of this thesis is to show that anthropogenic aerosol sources are affecting the microphysics and therefore the albedo of maritime stratus clouds.

In June 1994, The Monterey Area Shiptrack (MAST) Experiment was conducted off the California Coast to examine a phenomenon, first noted with the advent of TIROS satellites, known as Shiptracks. These areas of cloud brightening detected in the early TIROS images were suspected to be formed by additional aerosol produced by ships (Conover, 1966). An obvious motivation of this experiment was to be able to understand and quantify the environment in which shiptracks are formed. A less apparent, but equally important motivation of MAST was to attempt to understand how anthropogenic aerosol are modifying cloud reflectivity and thereby shed insight into the global radiation balance. Alterations in cloud albedo that occur through some type of microphysical change due to aerosols is an indirect radiative effect; indirect theory will be discussed further in Chapter II.

Aerosols that flow off continent increase the albedo of effected cloud regions -- shiptracks are not visible in these regions due to the high background CCN numbers. In contrast, air that has not been continentally influenced has relatively low CCN and thus, is more susceptible to shiptrack effects. These tracks result from increases in CCN from surface ships, as discussed previously in detail by Coakley *et al.* (1987). The formation mechanism is analogous to regional cloud brightening caused by continental flow, but the

scale is significantly smaller. Figure 1 illustrates an overall view of the different effects that continental and maritime flow regimes have on stratocumulus cloud region.

1. Aerosol Effects On Electro-Optical Devices

The Military has increased its use of electro-optical devices (e.g., television, low-light television, infrared, laser) for weapons systems, intelligence gathering and communications significantly over the past few years focusing considerable attention on the atmospheric factors that effect the performance of these systems. Physicists and meteorologists have been studying atmospheric effects on a variety of wavelengths in the electromagnetic spectrum for some time. The performance of high energy lasers, infrared seeking missiles and smart bombs, and infrared surveillance detection can be seriously affected by the loss of energy (from interaction with the beam) due to absorption and scattering of atmospheric molecules and aerosols. The uneven distributions of aerosols can have a significant effect on weapons systems applications (e.g., infrared wavelength ranging and imagery systems) as illustrated by Milton *et al.* (1987). Problems with propagating laser beams through the earth's atmosphere are addressed by Bloembergen *et al.* (1987), who point toward the absorption and scattering of atmospheric aerosols, including rain and fog as a major source in degradation of optical beam quality, thus power delivered, in ground based lasers. Cordray *et al.* (1977) consider several meteorological factors when correcting for an "aerosol-laden air mass;" one of which calls for multiplying aerosol density by a factor of two when there are continental trajectories for three or four days. The U.S. Navy has renewed its emphasis on the littoral regions of the world -- many of which are in close proximity to third-world industrialized zones where urban aerosol can make matters even more complicated. Thus, the operational battlefield success rates for electro-optical weapons systems would be greatly enhanced with better knowledge of aerosol amounts, locations and characteristics.

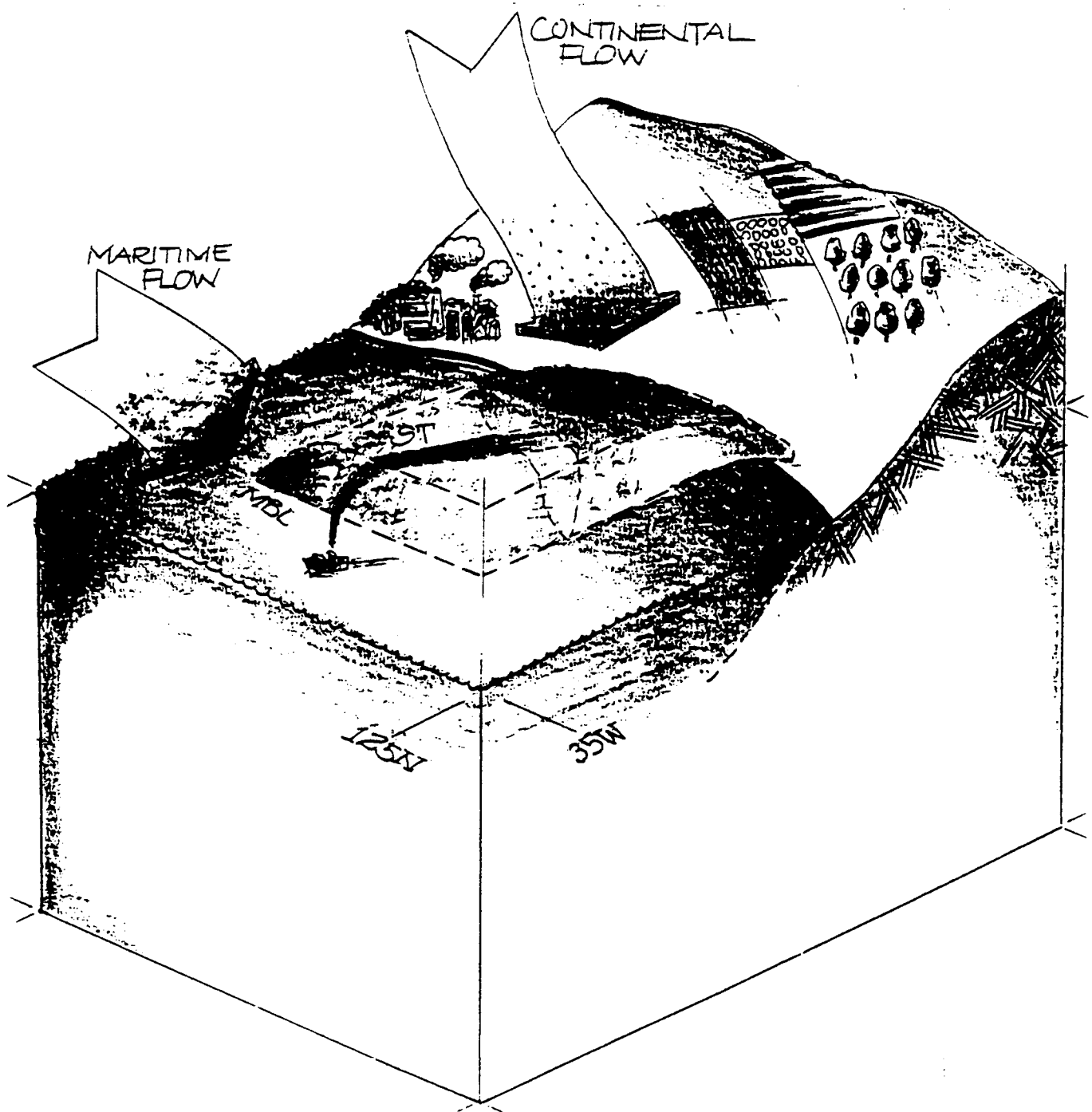


Figure 1. Coastal aerosol influence illustration depicting different effects that continental and maritime flow regimes have on stratocumulus cloud regions. The area of stratocumulus cloud influenced by anthropogenic aerosol does not exhibit shiptracks due to increased reflectance. A shiptrack is visible in the area of stratus further offshore that is influenced by maritime flow.

2. Aerosol Effects On Climate

Atmospheric aerosols and clouds can absorb and scatter solar radiation causing dramatic impact on the earth's energy balance and altering climate. The majority of global warming fervor has focused on increases in greenhouse gasses, like atmospheric carbon dioxide. The highly dynamic nature of aerosol volume, height and composition changes that has kept this important quantity from inclusion in many global climate models. Yet, it is commonly accepted that mean cloud albedo is a key parameter in climate regulation. Hansen *et al.* (1984) compared cloud albedo effects to carbon dioxide effects with a complex three dimensional climate model which included several atmospheric and oceanic feedback parameters. They reported a similar amount of warming ($\sim 4\text{K}$) for a two percent increase in solar irradiance as a doubling of carbon dioxide, suggesting two percent increase in planetary albedo could offset the carbon dioxide increase.

Brightening effects appear to influence optically thin clouds while absorptive effects are more significant in optically thick clouds, thereby suggesting an increase in global pollution could simultaneously brighten thin clouds and make thick clouds appear darker (Twomey, 1984). High cirrus clouds could abet global warming through absorption of long-wave terrestrial radiation. Even land-stripping, biomass burning and volcanic eruptions have been shown to be potential planetary sources for climate change. The focus of this thesis deals with cloud brightening of optically thin marine stratoform clouds -- a proposed major cooling mechanism for regulating the earth's climate. Aerosols can affect climate directly by backscattering solar radiation (Charlson *et al.*, 1991) or indirectly by increasing the number of CCN which leads to more cloud droplets with smaller radii. These smaller, more numerous particles may form a higher albedo cloud mass, thereby indirectly reflecting more solar radiation away from the earth. The indirect forcing mechanism may also have an effect on the longevity of stratus clouds if precipitation processes are affected (Albrecht, 1989) as shiptracks have been known to persist for up to 48 hours.

B. MONTEREY AREA SHIPTRACK (MAST) EXPERIMENT

MAST was a joint U.S.-British effort operated out of the Naval Postgraduate School designed to analyze the shiptrack phenomenon and a variety of hypotheses in four separate categories:

1. aerosol/cloud interactions and detailed microphysics
2. boundary layer perturbations by ships
3. cloud dynamics
4. background environmental conditions

Sponsored by the Office of Naval Research (ONR), this experiment included U.S. Navy ships, the National Aeronautics and Space Administration's (NASA) high flying ER-2, the research vessel Glorita, a Royal Air force C-130, University of Washington's C-131 and a Naval Research Lab (NRL) Airship. Satellite data was provided from the National Oceanographic and Atmospheric Administration (NOAA-9/10/11/12) Advanced Very High Resolution Radiometer (AVHRR) and Tiros Operational Vertical Sounder (TOVS) and Defense Meteorological Satellite Program (DMSP) (OLS, SSM/I, SSM/T) polar orbiters. Processing data from both platforms was conducted on site, at the Naval Postgraduate School. The time frame selected for the experiment, June 94, was chosen in anticipation of maximum status clouds -- the ideal cloud type for shiptrack formation and larger scale anthropogenically forced brightening. Figure 2 depicts the MAST operating area. Details for the experiment can be ascertained from the MAST Science Plan.

MAST hypotheses that relate to cloud dynamics and background environmental conditions include: 1) cloud reflectance and liquid water content (LWC) changes influence the radiation balance creating circulations that stabilize and confine the shiptrack region as a radiation-forced dynamic cloud and 2) shiptrack formation requires a set of background conditions which involve small boundary layer depth, CCN concentration below a given threshold, and pre-existing cloud formation mechanisms. The knowledge of shiptrack development has made great strides since their discovery by Conover in 1966. Once theorized as clouds left from missile range testing, the scientific community has limited

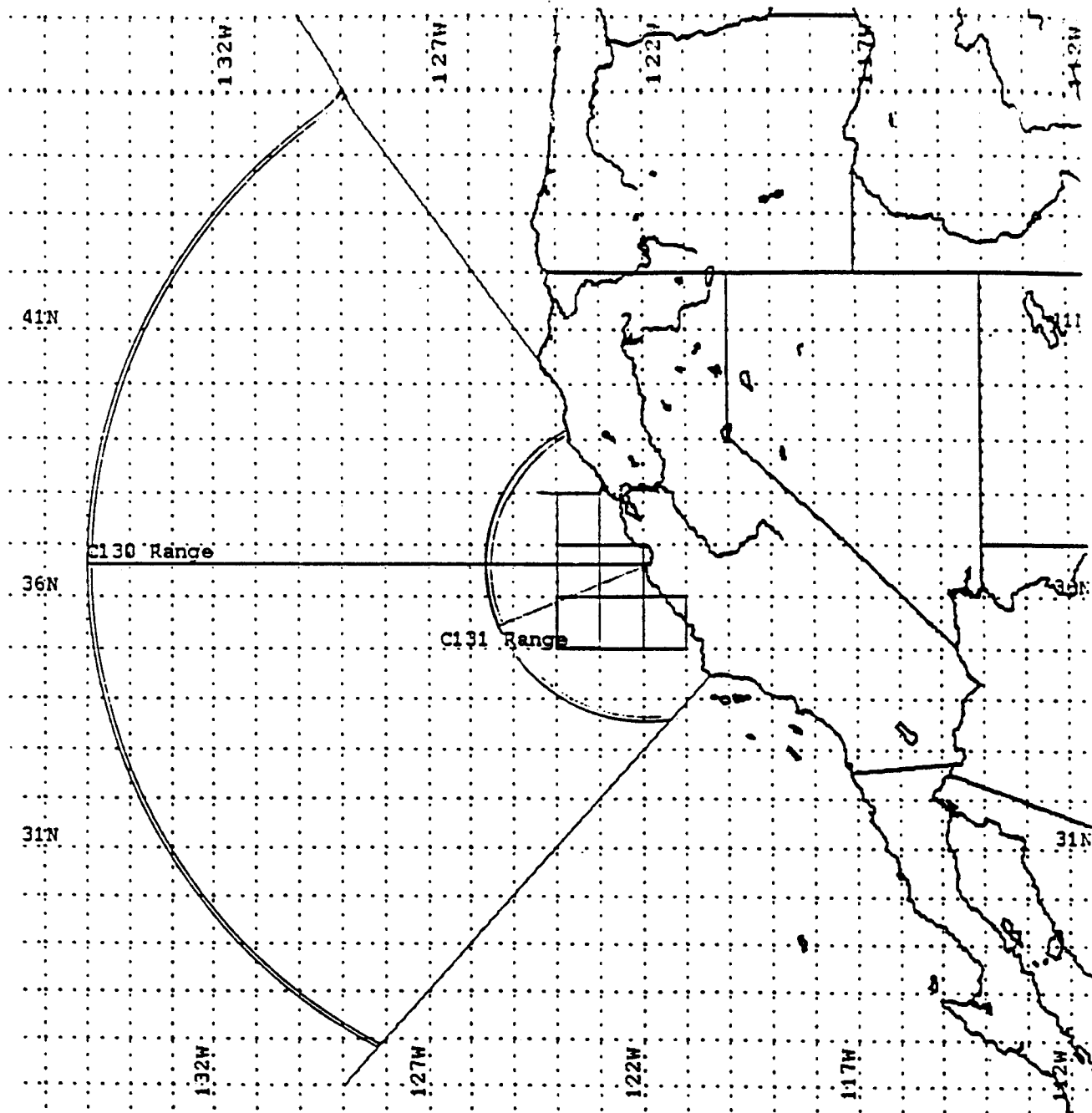


Figure 2. MAST Experiment 1994 Operations Area.

shiptrack development causal to sea salt generated by an ocean going vessel's turbulent wake or the byproducts of marine engineering plant combustion. However, the ambient conditions into which these aerosols are injected do not always result in the stratus cloud top shiptrack signature. Narrow ranges of sea surface temperature, humidity, marine boundary layer (MABL) height and background aerosols are the major environmental components that affect shiptrack development. Boundary layer height is considered to be the most important parameter, yet early analysis of MAST data has shown shiptrack occurrence in boundary layers from 100m to 800m. The most conducive shiptrack MABL seems to be approximately 500m (Trehubenko, 1994). Because not all 500m MABL's contain shiptracks, there must be other important factors that inhibit or foster shiptrack development. Background type, volume and composition of aerosol may be these other vital components.

C. CLIMATOLOGY OF STRATUS

Low level stratoform clouds dominate the marine environment. Klein and Hartmann (1993) describe the typical dynamical conditions associated with this cloud type as follows: stratoform clouds are generally found on the east side of marine subtropical highs where trade winds blow toward the intercontinental convergence zone (ITCZ) from the midlatitudes. Clouds form beneath a strong capping inversion over relatively cool sea surface temperatures (SST). Stratoform convective processes are held to the boundary layer through the descending side of a Hadley cell. When trade wind air masses advect toward warmer SST's near the ITCZ, the inversion tends to break apart making way for convective cumuloform development.

When these semipermanent highs discussed above have light winds and strong inversions, in close geographic proximity to littoral regions, the stage is set for possible pollution events. West Coast continental areas within 40 degrees latitude of the equator are most susceptible. During summer months (MAST time frame), trade wind inversions and light winds are present almost continuously unless disturbed by storms, fronts and associated cool air masses. These disturbances, found more frequently during winter time, can break up

the anticyclonic influence breaking up stratus and the conditions that foster air pollution episodes. During the MAST Experiment, only one synoptic scale low pressure system significantly affected stratus clouds on the 13th of June and the effects of this anomalous weather are highlighted in the Case Studies Section. It is important to note that while there have been extensive studies on stratoform cloud meteorology and air pollution events, few studies have attempted to link the two through trajectory analysis on a continental scale.

II. THEORY

A. AEROSOLS

Atmospheric aerosol have a broad range of sources. Hobbs (1993) classifies two major sources of these as: surface sources which occur at the bottom of the atmosphere and spatial sources which are present throughout the atmospheric volume. Surface sources include: biogenic and particulate matter, volcanic effluents, oceanic (i.e., primarily salt particle ejection) and fresh water aerosols, particulates from the earth's crust and those from biomass burning (which also include significant amounts of gasses that can form aerosols through gas-to-particle conversion, addressed in the next group). Spatial sources are produced in the atmosphere by widespread precursors such as: gas-to-particle conversion, cloud processes and extraterrestrial materials. Estimates of global strengths of these aerosols suggest clouds may be the major source of natural aerosol for particles with radii larger than $0.1\mu\text{m}$ (Hobbs, 1993).

Atmospheric aerosol are frequently categorized by size ranging from $.001\mu\text{m}$ for small ions up to $10\mu\text{m}$ for surface sources (i.e., dust, salt and combustion particles). Cloud droplets can be larger, usually between 1 and $100\mu\text{m}$. Aerosols with important optical parameters vary between $.01$ and $10\mu\text{m}$ and are present in greatest quantities in the lowest kilometers of the troposphere. The temporal scale at which aerosol can remain suspended is a widely debated topic which requires greater study. Time scales vary with changing meteorological conditions and type of aerosol allowing suspension from a few hours to many days. Aerosols can travel thousands of kilometers during their brief life spans undergoing chemical and physical changes including wet and dry deposition, coagulation, condensation, scavenging, mixing and dispersion.

1. Anthropogenic Aerosol

Urban aerosols are generally considered to be particles limited to $.001\mu\text{m}$ and greater. The sources and relative climatic importance of anthropogenic aerosol were recently reviewed by Andreae (1994). They include: sulfates from sulfur dioxide emitted from industrial

processes (burning fossil fuels), black carbon from vehicle exhausts and biomass burning, organic particles from biomass burning (deforestation and farming), nitrates from gasoline and oil consumption, dust and soil from agricultural practices, desertification and natural causes (Fig. 3). Sources of continental aerosols are exceedingly diverse and almost impossible to quantify. In general, anthropogenic aerosols are smaller and more numerous than marine aerosols like sea salt. The differences between continental and marine aerosols, in terms of principal aerosol-cloud interactions, are nicely depicted in Figure 4, a schematic from Hobbs, 1993.

B. CLOUD PHYSICS

1. Cloud Condensation Nuclei (CCN)

Water droplets form in the presence of atmospheric aerosols at supersaturations of about 2 percent (102% relative humidity) or less (Hobbs, 1993). This supersaturation is caused by adiabatic cooling, radiative cooling or cooling by conduction. The concentrations of cloud droplets are dependent upon the maximum supersaturation achieved and the number of CCN. This implies that as the supersaturation increases so does the number of CCN in the marine environment. Peak supersaturations in marine clouds are greater than in continental clouds, therefore continental air contains higher concentrations of CCN and higher droplet concentrations. Assuming the liquid water content of continental and marine clouds is similar, the average droplet size of continental clouds should be smaller than for marine clouds (Hobbs, 1993).

Several observational studies have shown the effects of anthropogenic CCN on cloud microstructures. Paper mills produce copious amounts of large CCN ($> .1\mu\text{m}$) and have shown an increase in cloud droplet concentrations downwind of the source (Hindman et al., 1977). Warner and Twomey (1967) showed an additional source of CCN caused by biomass burning during harvest season cane fires in Australia.

In 1993, Kaufman and Nakajima showed the effects of Amazon smoke particles on cumulus and stratocumulus clouds during the biomass burning season in 1987. Smoke

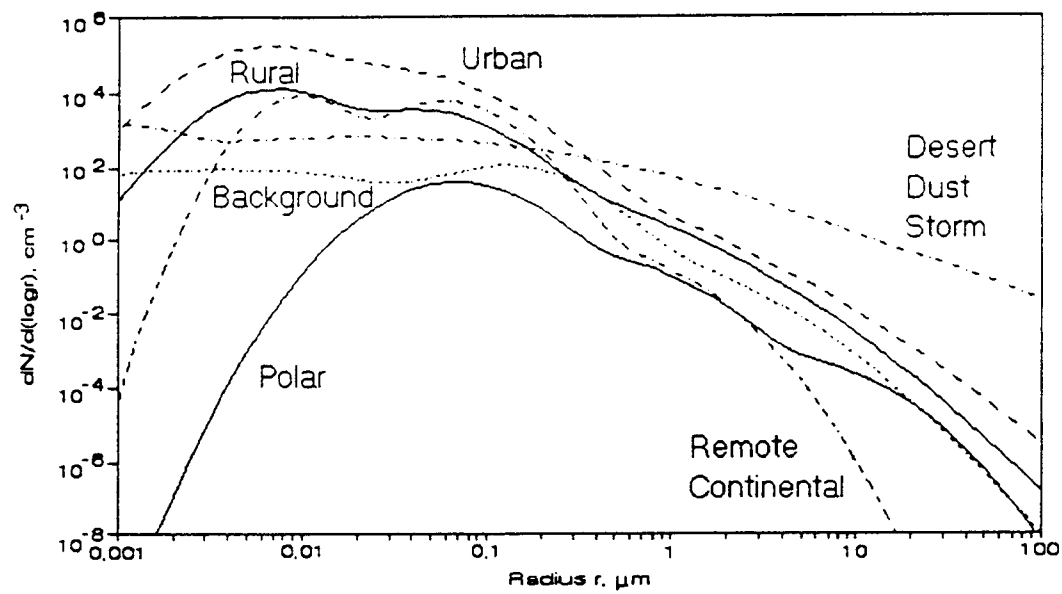
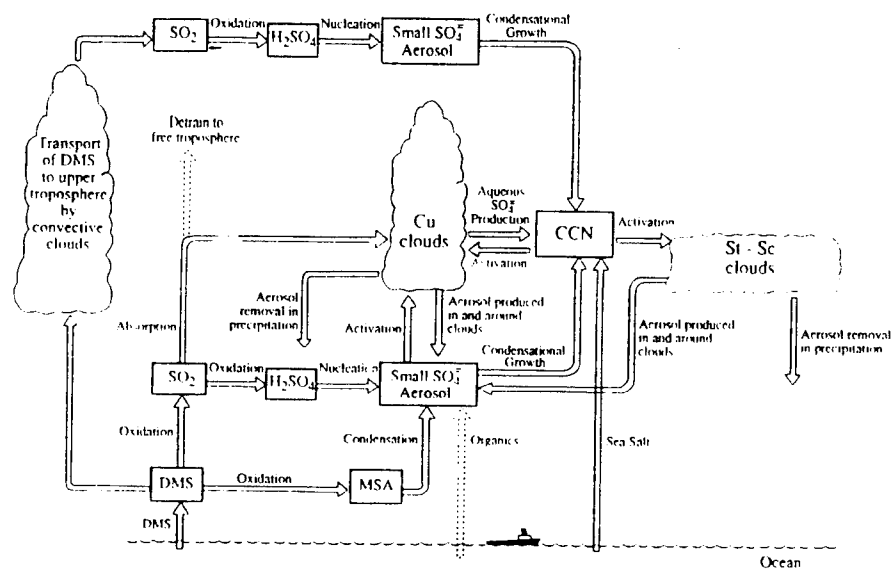
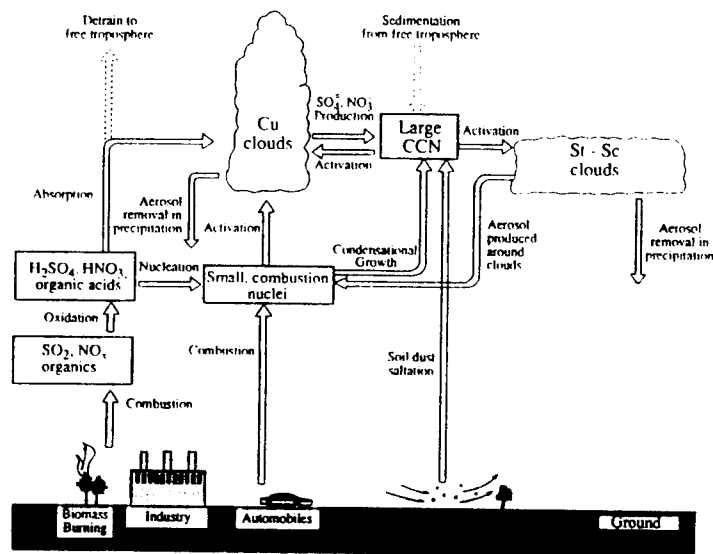


Figure 3. Size distributions of selected atmospheric aerosols (from Hobbs, 1993).



(a)



(b)

Figure 4. Schematic summary of principal aerosol-cloud interactions in (a) marine air and (b) continental air (from Hobbs, 1993).

particles scatter photons and serve as CCN in a similar fashion to sulfate effects (Radke et al., 1989), but perhaps do so with less complex interactions. Sulfur dioxide is converted into sulfate particles in dry air within the cloud mass over a period of several days, while smoke particles are generated close to the fire source from organic gas condensation. Therefore, the effect of smoke on clouds can be used as an experimental example of anthropogenic aerosol effects on clouds in general.

There are two opposing effects in regard to biomass burning, that can in concept be applied to fossil fuel usage. The first is a direct consequence associated with greenhouse gas emissions (carbon dioxide) causing a warming trend. The second effect causes cooling directly by solar radiation backscattering (Charlson et al., 1991) and indirectly by increasing CCN concentrations yielding smaller, more numerous cloud droplets which increase cloud albedo. It is this second indirect effect of droplet modification that is of primary concern in this thesis. Put more succinctly, we hypothesize that: urban aerosols enter the marine environment, stratus cloud CCN counts increase while droplet radii decrease, resulting in cloud brightening observable through remote sensing techniques.

C. RADIATIVE PROPERTIES

1. Reflectivity

Electromagnetic solar radiation that encounters atmospheric aerosols, clouds, water vapor, ice crystals, and assorted molecules is either attenuated or transmitted through the atmosphere. Attenuation of particles which are much smaller than the radiant energy wavelength are described by Rayleigh scattering. Rayleigh scattering efficiency is inversely proportional to the fourth power of wavelength. If the wavelength is proportional in size to the particle radius, the scattering process is governed by Mie theory (Liou, 1980). Mie scattering mechanisms govern cloud reflectance for this research.

2. Low-Cloud Reflectance at AVHRR Channel 3

The satellite data used in this thesis are from the polar orbiting NOAA-9, 10, 11 and 12 AVHRR satellites. AVHRR channel 3 was the primary channel utilized to determine low-cloud reflectance. Channel 3 was selected due to the fact that absorption plays a role in the near infrared (NIR) which encompasses $3.55 - 3.93\mu\text{m}$ (considered $3.70\mu\text{m}$). Reflectance from visible wavelengths, such as AVHRR channel 1 ($.63\mu\text{m}$), is dependent upon droplet size, liquid water content and cloud thickness. AVHRR channel 3 reflectance is dependent upon droplet size only (assuming cloud thickness greater than 100m). The single scatter albedo (the ratio of scattering to absorption for a single scatter episode) in the near infrared (NIR) is equal to 0.85 as compared to a value of 1.0 in visible wavelengths. Therefore, it is apparent that the absorption component of the single scatter albedo will influence backscatter as a function of droplet size in an inverse relationship. This concept of aerosol effects on cloud radiative properties is explored in further detail in Mineart, 1992.

3. Anisotropy

Anisotropy has to do with the angle formed between the satellite and sun which can cause a brightness change between images resulting in a cloud brightening bias. This brightening bias was observed during initial satellite analysis after the MAST experiment and it was decided that a change in the imaging process was necessary. Corrections to anisotropy are intended to remove angular effects of reflecting surfaces (i.e., low-level clouds). The anisotropic reflectance factor (ARF) corrects for the specific angular geometry between sun, surface and satellite for each pixel. The process is initialized with a variety of parameters including cloud size distribution (standardized for stratus climatology), wavelength ($3.7\mu\text{m}$), and composition (refractive index). These parameters are then input into numerical Mie code. Next, phase function corrections are made and combined with solar irradiance for input into a discrete ordinate radiation transfer program with a numerical 24-stream solution. Radiance intensity values are computed for satellite zenith angle, sun zenith angle, and relative azimuth and double integrated with a bidirectional reflectance equation (for a small surface element). Finally, the ARF is available in table form.

III. METHOD OF DATA ANALYSIS

A. OVERVIEW

Synoptic weather patterns were analyzed to ascertain time frames and areas most conducive to comparison of marine and continental effects on stratus formation. A brief daily synopsis of weather patterns and low level flow is provided in the Appendix. NOAA-9, 10, 11 and 12 AVHRR daytime satellite imagery was analyzed to locate "dirty" cloud regions that were brighter than their surroundings possibly due to an influx of continental aerosol. Less bright, "clean" regions, frequently exhibiting shiptrack effects, were also located from the imagery. These lower reflectance regions are characterized by fewer aerosol and CCN. Section B discusses the display schemes utilized through the TereScan software; AVHRR channel 3 was the primary tool as it is best for depicting low level cloud reflectance. Anisotropy corrections were applied at all display stages.

After analyzing satellite imagery from the NOAA polar orbiter passes, a long-range transport and dispersion trajectory analysis model was employed (see HY-SPLIT Model discussion below in Section C.). A "dirty" region of stratus is characterized by increased reflectance values (greater than 20 percent on a scale of 0 to 50) and few, if any, discernable shiptracks. Back trajectories were run from the "dirty" cloud masses from a minimum of three different points, at different heights above and below the boundary layer. A similar technique was employed for "clean" cloud areas. "Clean" stratus cloud have lower brightness values (less than 15 percent) and are marked by the presence of shiptracks. Forward trajectories from urban locations coinciding with major cities (e.g. San Francisco, Los Angeles, Portland, etc.) were also run to try to show consistency between possible anthropogenic sources of "dirty" stratus. The Case Study section (Chapter IV) will illustrate the different reflectance values of stratus clouds and how the trajectories are classified.

B. SATELLITE RETRIEVAL TECHNIQUE

The retrieval technique involves a variety of steps and assumptions (simplification assumptions for stratocumulus cloud pixels made in radiative balance and throughout the retrieval process). The basic steps are as follows: 1) 'avin' creates TereScan AVHRR sensor datasets from high-resolution picture transmission (HRPT) telemetry data from storage tapes. 2) 'avcal' converts AVHRR sensor count values to values with engineering units. For channels 1 and 2 units are in percent albedo (a pre-launch linear relationship converts raw counts to percent albedo). Channels 3, 4 and 5 are in brightness temperatures or radiances, based on a linear relationship that converts cold space raw counts (~3K) to raw counts associated with an onboard target (~280K). Infrared radiances are converted to temperatures using an inverse Planck function. 3) Finally, a set of programs called 'upick' allows the user to pick a set of AVHRR products to be extracted from raw HRPT telemetry data. For each satellite pass selected a TereScan dataset (tdf) is created which includes the following 4 products utilized in this study:

1. 'cldtyp' - a cloud type pixel classifier that is always an output.
2. 'low1' - low cloud reflectance; channel 1 ARF(see subsection *b.*) applied.
3. 'ref3' - low cloud reflectance; channel 3 ARF not applied
4. 'low3' - low cloud reflectance; channel 3 ARF applied and updated each julian day for low clouds.

Composites are available for some products; low3 composites of 5 days were used in Chapter IV, Case 2 and Case 3.

C. HY-SPLIT MODEL

There have been numerous pollutant transport models with a wide range of complexities introduced in the past few years. This thesis employs a hybrid between Eulerian and Lagrangian modeling approach called the Hybrid Single-Particle Lagrangian Integrated Trajectory (HY-SPLIT) model (Draxler, 1988). The HY-SPLIT model was developed in three stages: the first incorporated simple wind-shear driven dispersion (Draxler and Taylor, 1982), the second included separate daytime or nighttime mixing regimes (Draxler, 1982) and

finally the third stage with vertical mixing calculations that vary temporally and spatially (Draxler, 1987).

HY-SPLIT emits a pollutant source particle at a given x-component, y-component and pressure height. At two hour intervals, new u, v and w wind components are computed from the dataset. Vertical motion is determined by an integrated forward-differencing of the total derivative of pressure. Horizontal advection is computed by averaging winds at both the start and end of the advection step in order to calculate a transport vector. The entire source particle mass is contained at each particle position at the designated release point. As the particle position changes temporally, the pollutant volume centroid grows at a constant rate in the horizontal; vertical expansion is proportional to the square root of the mixing coefficient. Figure 5 is a two dimensional example of a forward trajectory run from San Francisco at 1000 meters elevation. This pollutant volume flows offshore around Big Sur into the Los Angeles Basin and continues to flow easterly over the Baja Peninsula. The pollutant is assumed to be uniformly distributed in all three directions (x, y and z) about the centroid. Sigma surfaces are used in the vertical and a simple Ekman boundary layer model is employed below the lowest sigma level. Winds in general are interpolated to appropriate levels for subsequent dispersion and transport calculations.

The latest windows version of HY-SPLIT was obtained from NOAA's Air Resource Laboratory (ARL). After considerable programming adjustment and modification the model became operational, in house, on an IBM RS-6000 workstation. Readers interested in more details of the HY-SPLIT model should consult NOAA Technical Memorandum ERL ARL-195.

Clearly one of the most important facets of dispersion models is the dataset. In general, the finer temporal and spatial resolution available, the more realistic the model output. The dataset employed is from the National Weather Service's National Meteorological Center (NMC) for the period of the MAST Experiment (1 - 30 June 1994). The primary operational system is the Regional Analysis and Forecast System (RAFS) which employs the Nested Grid Model (NGM) for its forecast. The data is referred to as NGM, because the forecast component of the system is from the NGM model. The NGM data was

START MONTH- 6 DAY-21 HOUR- 0Z

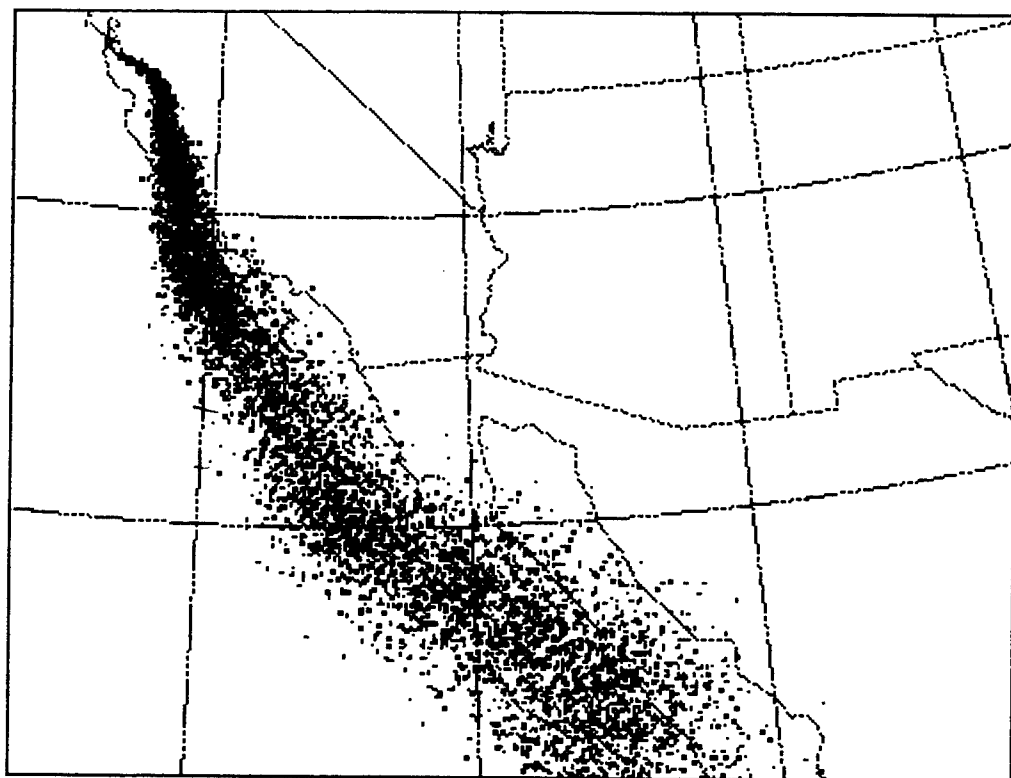


Figure 5. HY-SPLIT Model Forward trajectory run from San Francisco.

obtained from the NOAA Air Resources Laboratory (ARL) and is archived at 10 sigma levels ranging from 0.9823 - 0.43414 (approximately 980 - 434mb). ARL packing methods contain u and v wind components, temperature, humidity, and flux fields. ARL archives the data at two hour intervals on a 180km, 33 x 28 polar stereographic grid field covering the United States, Southern Canada and immediate coastal waters (the finer resolution one hour, 91km grid was not available).

IV. CASE STUDY RESULTS AND EVALUATION

A. CLASSIFICATION OF TRAJECTORY TYPE

Several case studies are discussed in order to better acquaint the reader with the synergistic relationship between trajectories, satellite imagery and meteorology. Not all of the trajectories used in these examples were included in the data analysis. For statistical purposes, backwards trajectories were broken down into three major categories:

1. 'Continental' trajectories pass over the coast at some point of travel yielding an offshore component that suggests continental air is flowing into the marine environment bringing with it a source of anthropogenic aerosol.
2. 'Marine' trajectories have no interaction with the continental landmass. This air is much cleaner with fewer CCN generating aerosol.
3. 'Continental influenced' trajectories do not flow directly over the continent but seem to feel the effects of the coastal environment. Influence trajectories can exhibit much greater curvature in the horizontal and more rapid descent in the vertical than marine trajectories.

Backward and forward trajectories were utilized for this study, but because forward trajectories require more assumptions, due to complex surface interactions, they are considered less reliable indicators of air advection.

The HY-SPLIT Model provides numerical output, as well as graphical display for a variety of parameters. These files were edited for input to a TereScan compatible program that allows the trajectories to be plotted directly over the satellite image. All of the satellite imagery onto which the trajectories are overlaid, are either NOAA 11 or NOAA 12 AVHRR channel 3 passes. Trajectories of interest are labeled by number at the point of latitude and longitude that coincides with the imagery overpass time to the nearest hour. A contrast bar

is located in the upper-left side of the image to assist the reader with brightness scale with values that range from 0 to 50 percent reflectance.

B. CASE 1 (11 June):

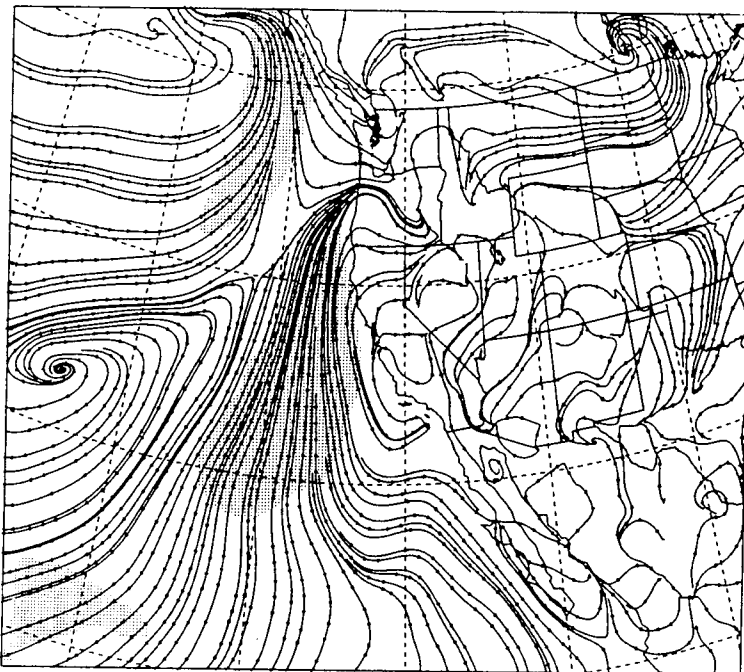
1. Synoptic Summary

The weather conditions for the week preceding Case 1 were typical of slow moving Pacific high pressure regimes. On 8 June, offshore ridging extended from 35°N/125°W into Idaho. The ridge begins to weaken on the 10th and tilt slightly northward. The trough axis shifts westward and geostrophic winds between the Pacific anticyclone and thermal low (over California's central valley) indicate offshore flow between Washington State and northern California; NORAPS streamline analysis confirms this at the surface and 925mb (Fig. 6). On 11 June, Pacific high ridging, eastward over northern California is still present and the thermal trough has shifted back toward the Central Valley and weakened. Stratocumulus develops and extends into the MAST operating area south of a line extending from 36°N/123°W southwest to 32°N/127°W. This line that separates clear air from bright stratus is a topic of some controversy. While this cloud-free region clearly separates dirty stratus to the southeast from cleaner cloud to the north (above the line 35°N/130°W to 40°N/126°W), it is surmised that this delineating clear region is actually composed of high numbers of continental aerosol with lower humidity. In these clear regions forecasters focus in on MABL height and look for the slightest lift in the inversion height to bring parcels to that minute saturation increase that triggers stratus formation.

2. Trajectory Synopsis

Trajectory 1 (T1) is located at 30°N/120°W in a fairly homogeneous area of dirty stratus (Fig. 7). The brightness value associated with this back trajectory is 25.5 percent. T1 was counted for statistical analysis in the continental flow, dirty cloud category. The closest clean cloud region is to the northwest, where the nearest shiptrack is located over 350km away.

sfc streamlines iso



925 mb streamlines iso

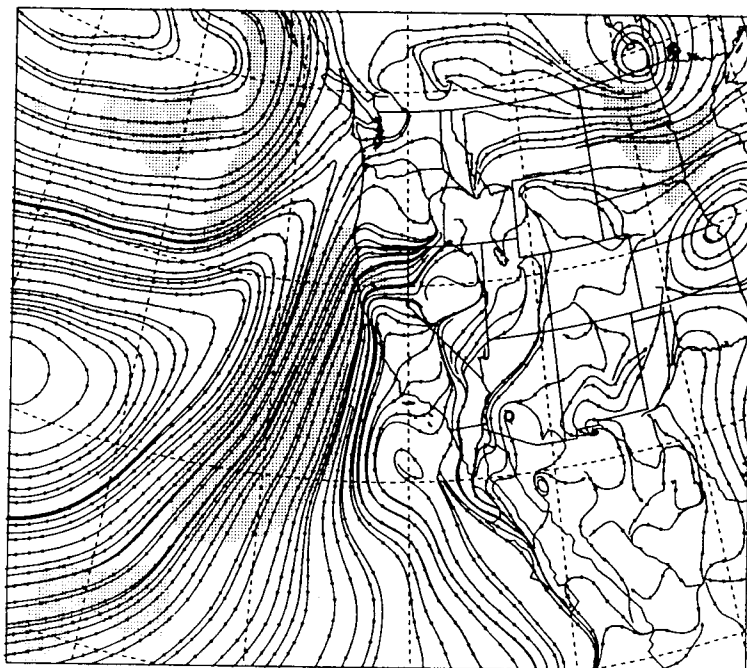


Figure 6. NORAPS Model streamline analysis 1200 UTC, 10 June 1994.

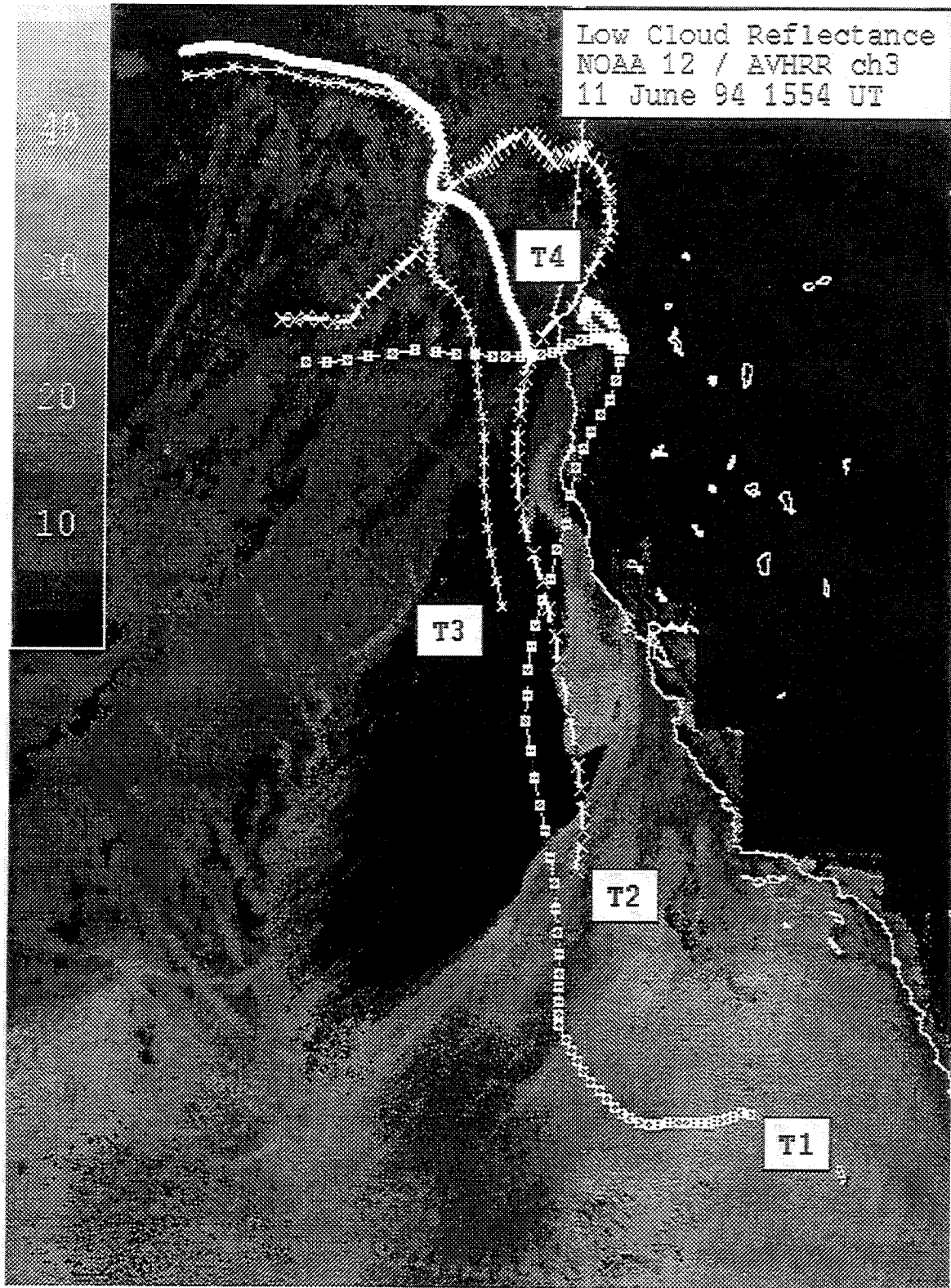


Figure 7. NOAA 12, AVHRR Channel 3 image from 11 June 1994 showing backward trajectories T1 (boxes), T2 (large crosses), T3 (small crosses), and T4 (heavy line).

Trajectory 2 (T2) is located due west of Point Conception at $35^{\circ}\text{N}/125^{\circ}\text{W}$. Although the cloud here is still relatively bright compared to the rest of the image, shiptracks are evident suggesting that the air mass is slightly cleaner than for T1. This continental trajectory was not included for statistical purposes as there is a clear region 80km to the north northwest. The fact that continental T1 and T2 flow off the California coast in the morning hours of 9 June correlates with NORAPS streamline analysis (Fig. 8).

Trajectory 3 (T3), located at $38.5^{\circ}\text{N}/125.5^{\circ}\text{W}$ shows westerly flow until 0600 UTC on the 10th, when the trajectory curves right, and heads toward the south into a vast region of clearing. It is theorized that these cloud free coastal regions are caused in part due to subsynoptic scale offshore flow. The smaller coastal brightening, approximately 100km off of San Francisco Bay is most likely an indication of mesoscale offshore flow. Possible sources of this small-scale brightening include sea breeze upper-level return flow and land breeze flow during evening hours.

Southwest of Cape Mendocino, trajectory 4 (T4) can be found in an area of clean stratus containing numerous shiptracks. These tracks result from increases in CCN from surface ships, as discussed previously in the introduction. T4 is clearly a marine trajectory -- exhibiting a steady northwesterly flow from the Pacific.

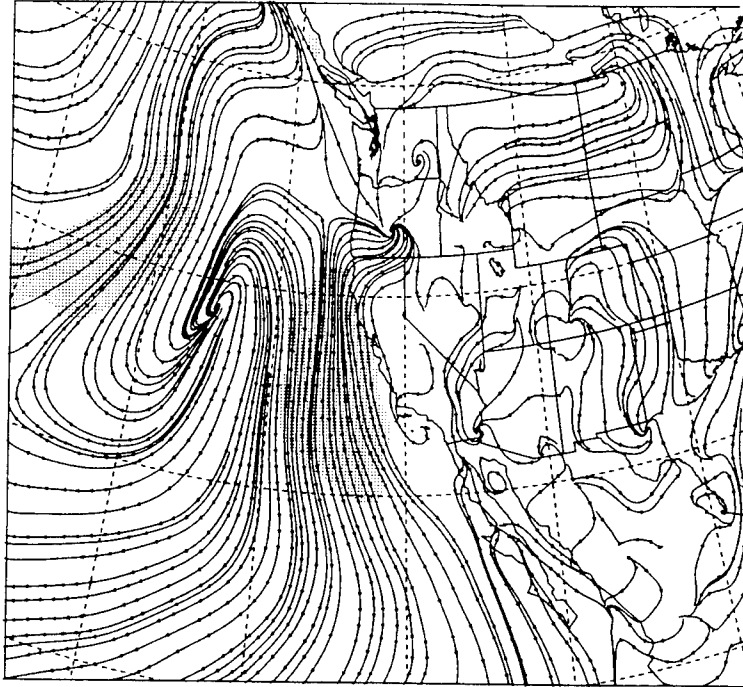
The difference between T1 and T4 help to define the extent of the continental air mass influence. Based on reflectance differences illustrated in Chapter II, the cloud region influenced by continental aerosol should appear significantly brighter than the clouds with strictly marine aerosol origins. The stratus in the immediate vicinity of the coast, as well as surrounding T1, has the brightest reflectance values in the image.

C. CASE 2 (13 June):

1. Synoptic Summary

This particular case was selected to illustrate the effects of large scale frontal features in influencing air flow and stratus. Weather previous to 12 June is discussed in Case 1. On the 12th, at 1200 UTC a surface low is located at $50^{\circ}\text{N}/140^{\circ}\text{W}$ with a central pressure of

sfc streamlines iso



925 mb streamlines iso

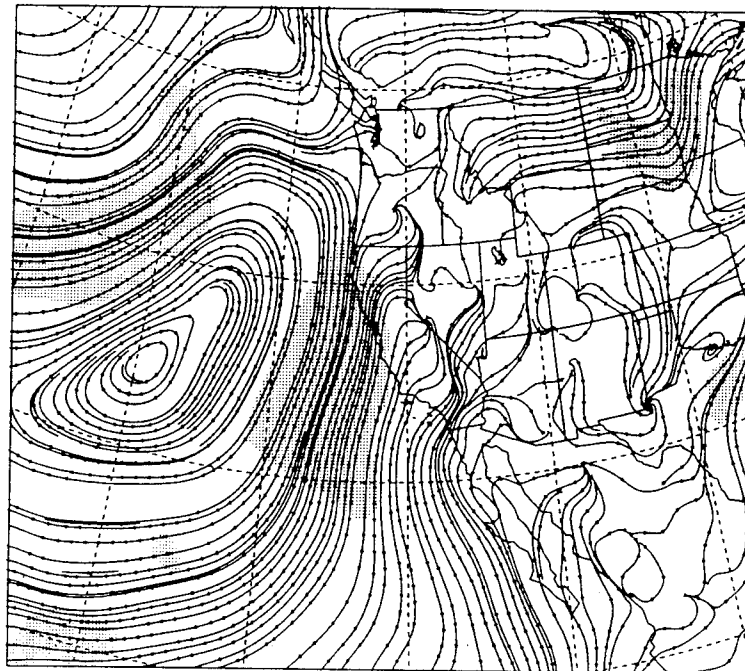


Figure 8. NORAPS Model streamline analysis 1200 UTC, 09 June 1994.

984mb. Figure 9 shows that by 13 June the low pressure system has closed to within 200km of Vancouver Island and central pressure has dropped to 983mb. The influence of this system is apparent in the cyclonic curvature off the west coast in Figure 10. The boundary between clean and continentally influenced cloud is located much further eastward toward the Baja Peninsula than typically observed during the MAST experiment.

2. Trajectory Synopsis

As shown in Figure 10, T1 is located at 30°N/120°W due south of Santa Cruz Island. Continental in origin, this trajectory reveals offshore flow from the San Francisco Bay area. Forward trajectories run from San Francisco are well correlated with the back trajectories. Figure 11. is a forward dispersion trajectory that is released at 1000 meters from San Francisco on June 10th at 1800 UTC. This simulated model release coincides with the approximate time and height that T1 passed offshore over San Francisco Bay.

Four hundred kilometers to the west north-west, T2 is located in a broad region of clean, non-continentally influenced air where many shiptracks exist. When comparing the linearity of these trajectories, one immediately notes how smooth T2 is compared to the erratic nature of T1. It can be inferred, from experience with the model, that as trajectories either approach or depart from the continental boundary they exhibit the effects of diurnal winds in the coastal environment.

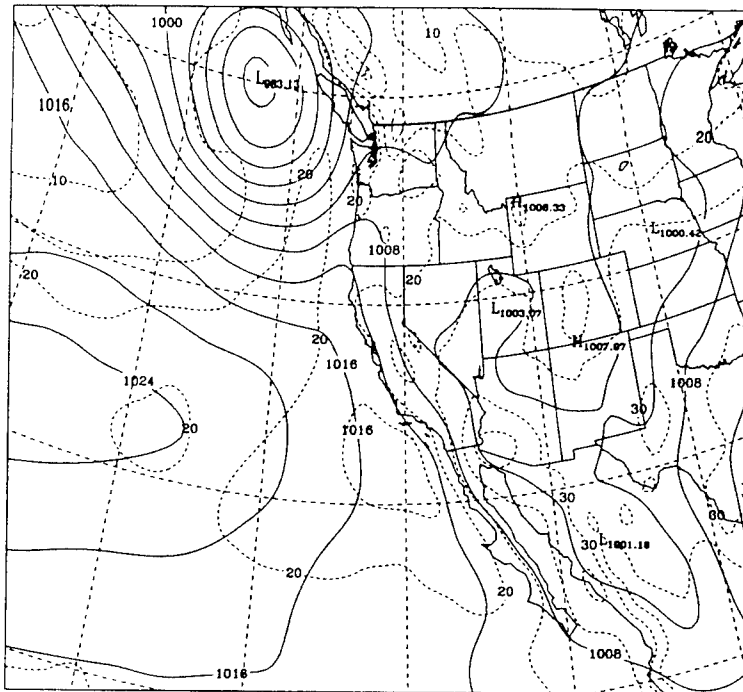
T3, located off Oregon's Cape Blanco is far enough north that it gets influenced directly by cyclonic curvature around the low and follows the frontal feature visible in Figure 10. This case study shows an example of an atypical synoptic scale, low-pressure region that is used to contrast with Case 3 below.

3. Additional Comments

Note, on Figure 10, the different trajectory lengths. T3 is shorter because it contains only one day of data, while the other two trajectories have a minimum of three days worth of data. T2 and T3 intersect just south of T3's start position. At this intersection point, T3 is 2 hours old with respect to the image pass time on 13 June, while T2 passed through two

0000Z 13 JUN 1994

slp t rh



925 mb ght t rh

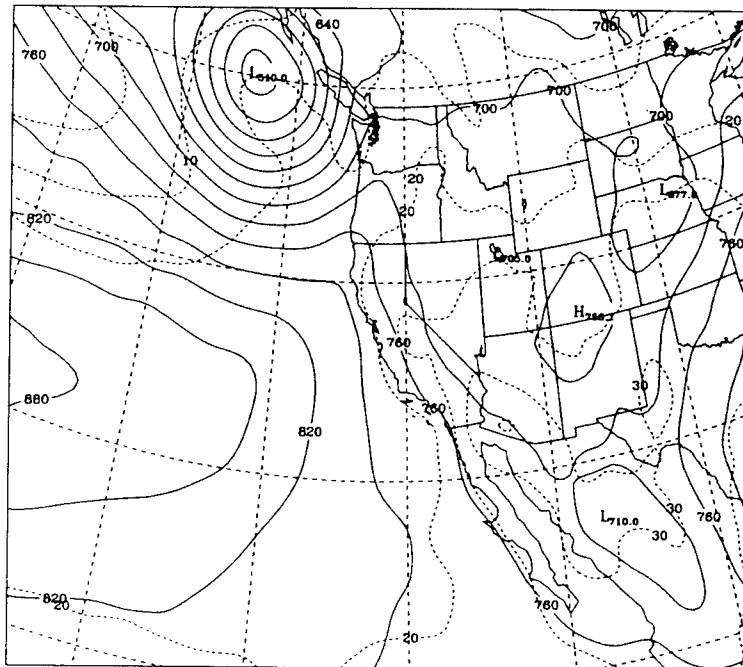


Figure 9. Low pressure center off Vancouver Island at 0000 UTC, 13 June 1994. Central surface pressure is 983mb. (NORAPS model analysis fields: sealevel pressure, temperature, humidity)

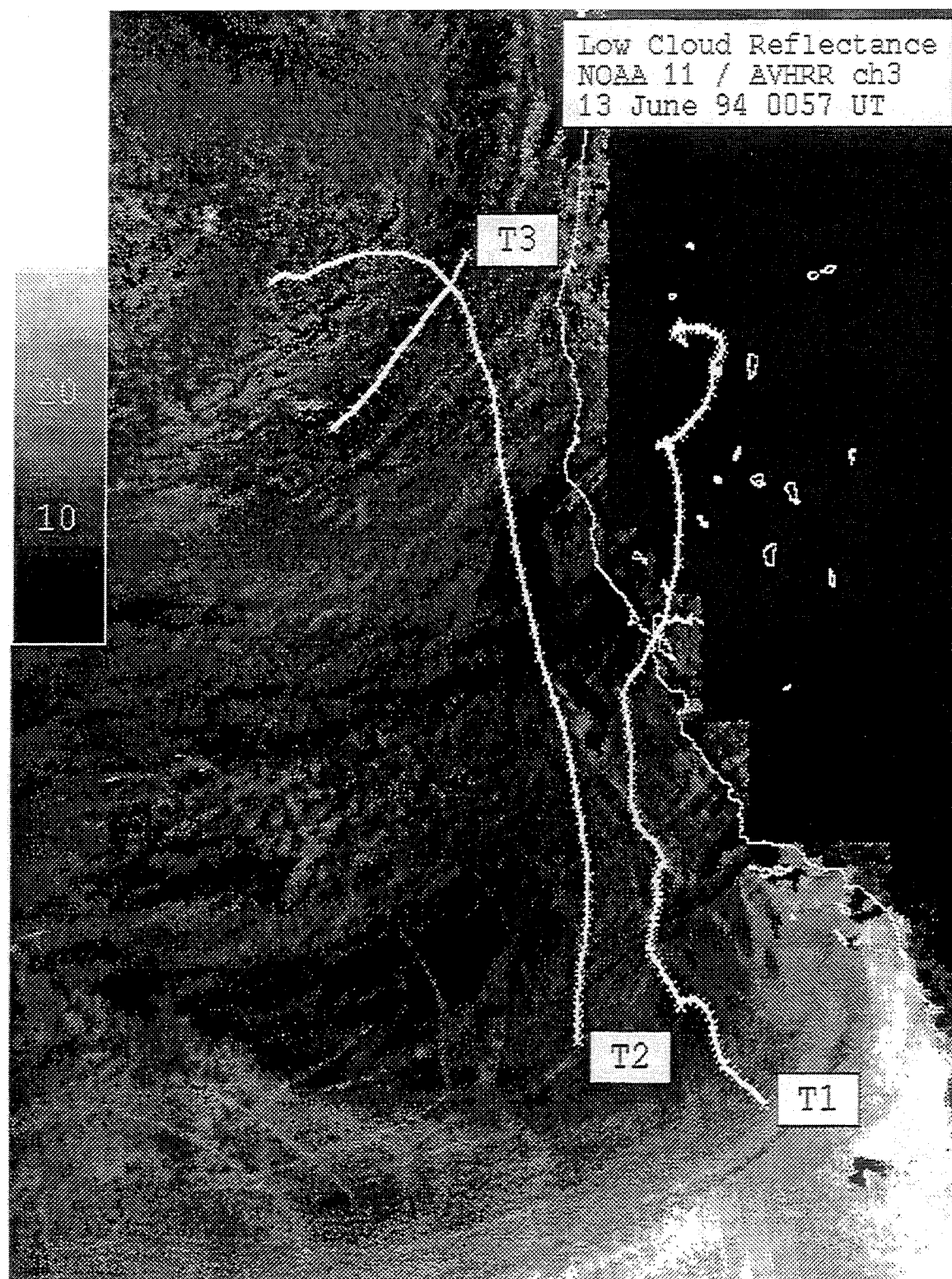


Figure 10. NOAA 11, AVHRR Channel 3 image from 13 June 1994 showing backward trajectories T1, T2, and T3.

START MONTH- 6 DAY-10 HOUR-18Z

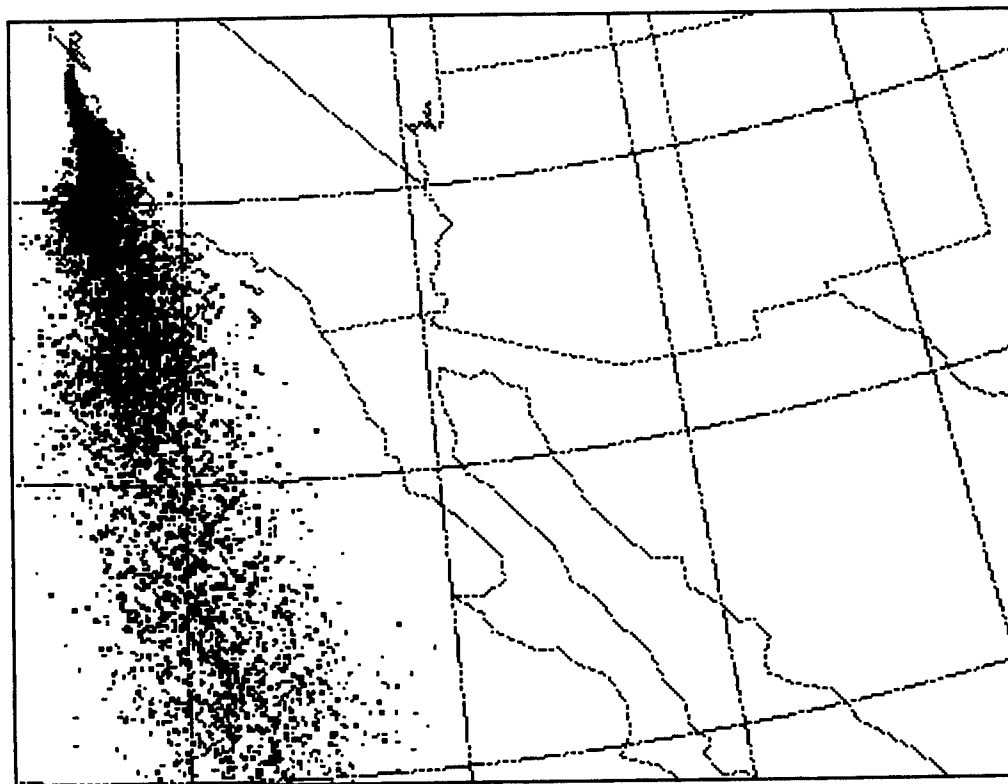


Figure 11. Forward dispersion trajectory released from 1000m on 10 June 1994, 1800 UTC from San Francisco. This trajectory is used to correlate back trajectories run on 13 June 1994.

days earlier on the 11th. The fact that these two trajectories cross orthogonally to each other at different times, highlights the low level flow pattern shift, from WNW on 11 June to SW on the 13th.

D. CASE 3 (21 June):

1. Synoptic Summary

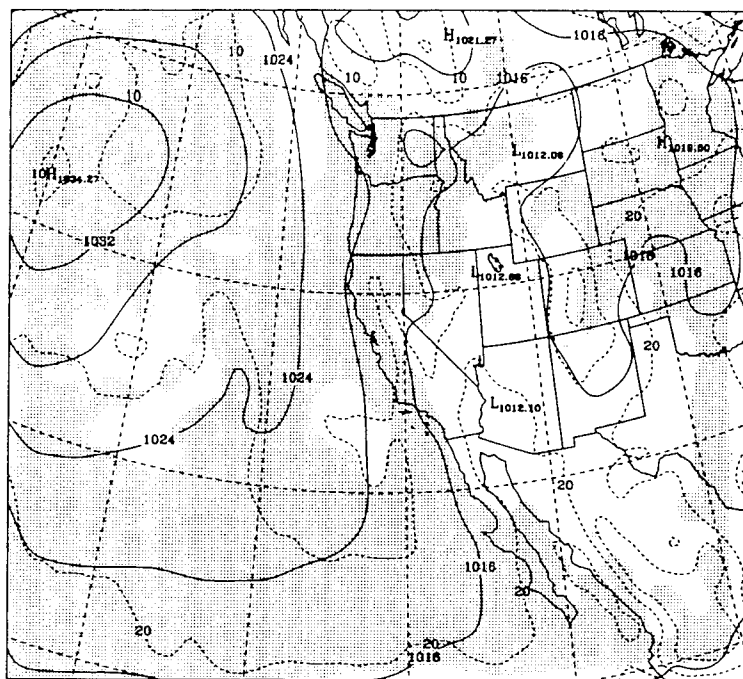
This particular case is representative of the more common synoptic weather encountered during the MAST Experiment time frame. These meteorological conditions are consistent with the summer stratus climatology discussed in Chapter I. The persistent feature that was dominant over the previous week is the Pacific anticyclonic high. It is located at $43^{\circ}\text{N}/150^{\circ}\text{W}$ on Figure 12 (21 June, 1200 UTC surface pressure analysis) and has associated broad regions of stratus sheeting. The stratus stretches from the eastern side of the anticyclone to the California coast, from San Francisco south along the Baja Peninsula, and is visible throughout most of the operating area as seen in Figure 13. For comparison purposes, T1, T2 and T3 are located at the same latitude and longitude for Case 1 and Case 2.

2. Trajectory Synopsis

Both T1 and T2 are located in the extensive region of increased reflectance. T1 is classified as continental and shows offshore flow from northern California. T2 is an excellent example of the continental influenced category of trajectory. As it approaches the Washington-Oregon State border the trajectory 'feels' the effects of the coastal environment and makes a nearly 180 degree turn within 70km of the coast. T3, located at $44^{\circ}\text{N}/126^{\circ}\text{W}$, exhibits more typical synoptic low-level flow from the NNW. Brightness values are lower here coinciding with the influx of clean, low CCN count air.

1200Z 21 JUN 1994

slp t rh



925 mb ght t rh

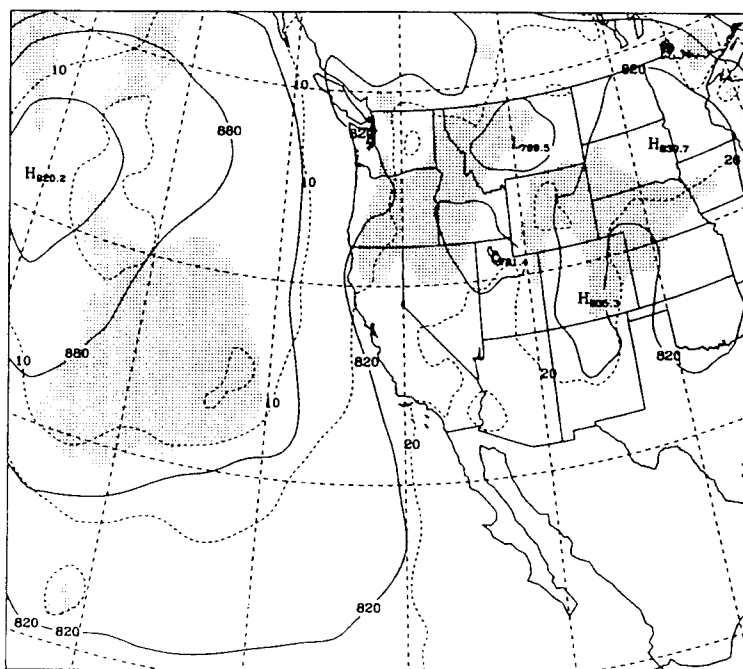


Figure 12. Typical synoptic condition in the eastern Pacific showing persistent anticyclonic high at 1200 UTC, 21 June 1994. (NORAPS model analysis fields: sealevel pressure, temperature, humidity)

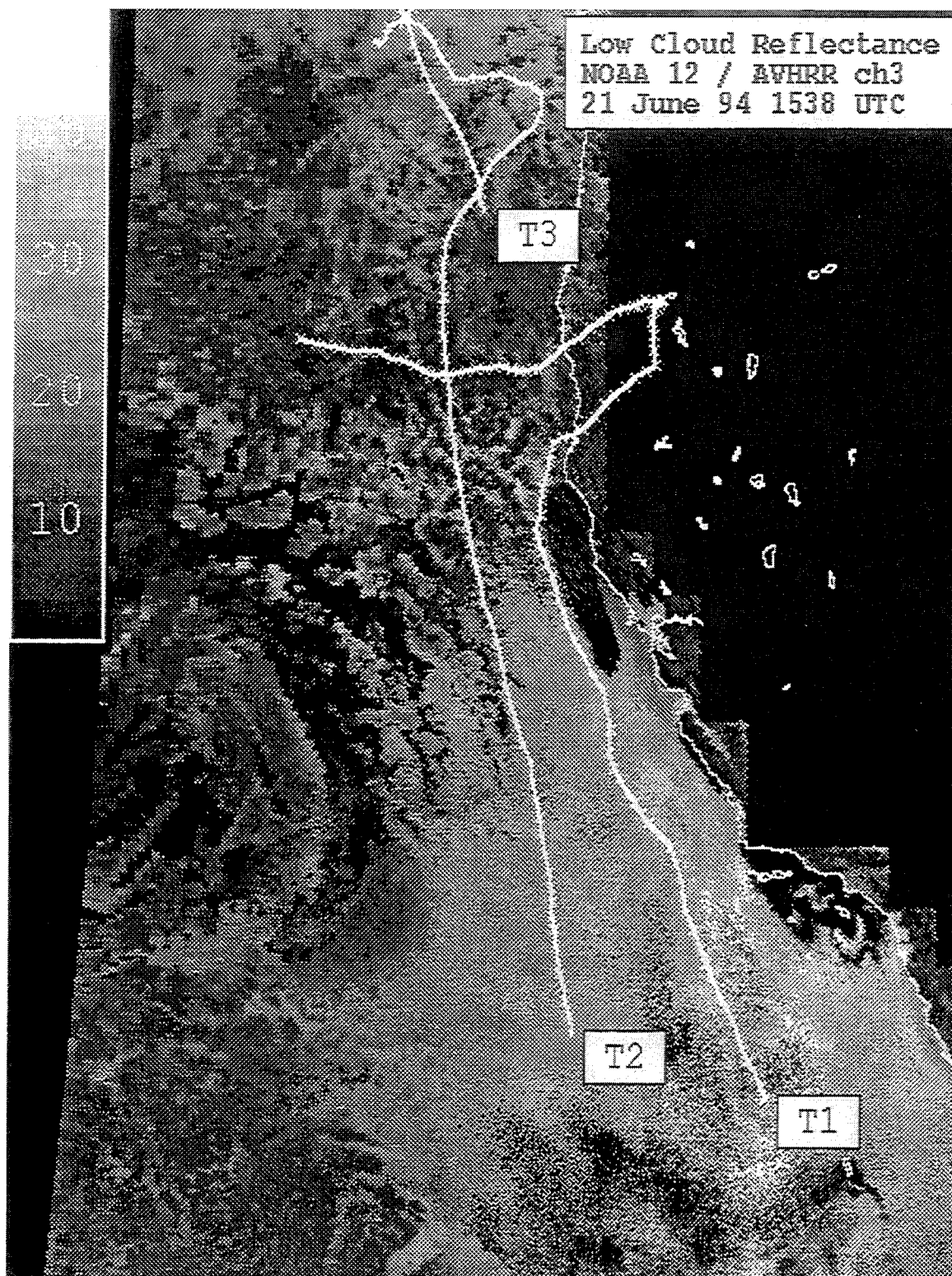


Figure 13. NOAA 12, AVHRR Channel 3 image from 21 June 1994 showing backward trajectories T1, T2, and T3.

3. Additional Comments

The continental/marine boundary that runs roughly along longitudinal line 128°W is apparent in the Figure 13. On the 13 June, channel 3 image (Fig. 10), this boundary is shifted dramatically to the east; the orientation of this delineation between continental and marine air mass runs southwest out of the Los Angeles Basin. There are no ship tracks visible in the region under the influence of offshore flow, as it is presumably saturated with continental CCN. A comparison of these two cases is addressed further in Section G.

E. CASE 4 (29 June):

1. Synoptic Summary

In the week preceding the 29th, weak transitory lows propagate through the dominant East Pacific high. High pressure builds into the Oregon/Idaho state boundary on the 26th of June. In the evening hours of 27 June, an elevated trough passes through north of the operating area; this relatively weak propagating feature provides just enough reduction of subsidence to cause the inversion to rise slightly, resulting in stratus formation. Stratocumulus clouds persist off the West Coast through the 29th of June.

2. Trajectory Synopsis

Figure 14 shows T1 as a prime example of a continental trajectory with offshore flow from Northern California. Anthropogenic laden air advects down the coast toward $30^{\circ}\text{N}/120^{\circ}\text{W}$ where reflectance percent values are approximately 20. T2 is in a less homogeneous area of brightening and represents the influence category of trajectory due to its proximity to land near the U.S./Canadian Border.

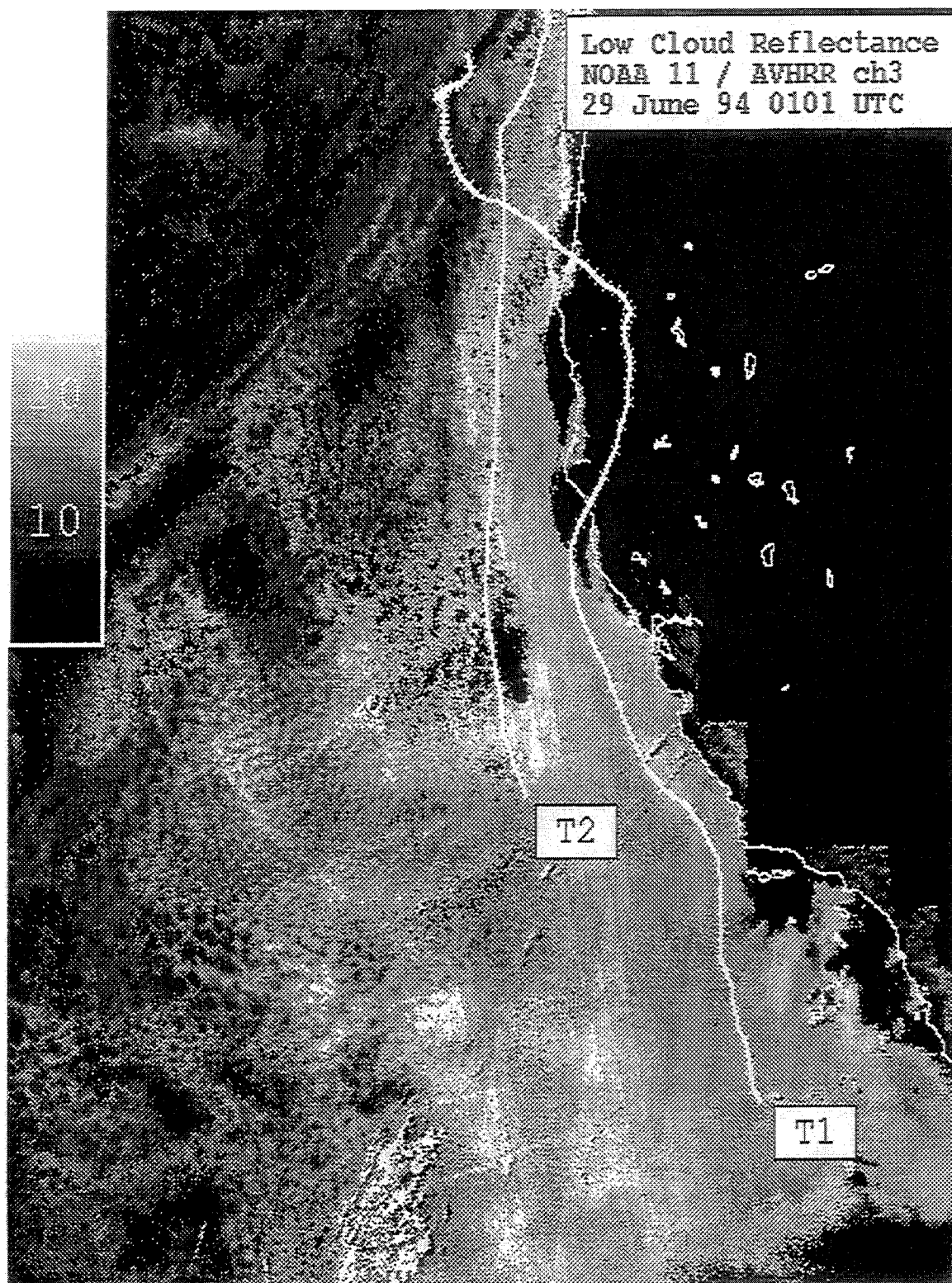


Figure 14. NOAA 11, AVHRR Channel 3 image from 29 June 1994 showing backward trajectories T1 and T2.

F. CASE 5 (June 30):

1. Synoptic Summary

The weather conditions on the 30th are quite similar to the previous day (Case 4) with little significant synoptic scale change. Streamline analysis of 29 and 30 June are remarkably similar as well. Yet, stratus begins to erode late in the day although no drizzle is reported. Regional analyses ten hours previous to each case respectively provide a possible explanation. Note, in Figure 15a, the stronger gradient and more easterly component of offshore flow between Northern California and Washington state on the 27th of June, as compared to the same analysis time on 28 June (Fig. 15b).

2. Trajectory Synopsis

T1, located at $30^{\circ}\text{N}/120^{\circ}\text{W}$ as shown in Figure 16, resembles Case 4, T1. Reflectance values of 22 percent confirm the offshore surface flow south of Cape Medocino. T2 is classified marine as it is not influenced significantly by the coast and maintains a distance of greater than 100km from land. The stratus clouds around $35^{\circ}\text{N}/125^{\circ}\text{W}$ are cleaner with much lower reflectance values around 10 percent. T2 suggests clean, low CCN volume air is advected into this region from the Pacific.

3. Additional Comments

Additionally, a thin bright coastal band of cloud within 150km of the San Francisco Bay Area (extending along 124°W) is located between the clean and clear cloud regions. This small scale littoral brightening is likely caused by anthropogenic aerosols that are probably carried offshore during evening land breeze conditions or return flow from sea breeze circulation. Another possible interpretation for channel 3 brightening effects is offered by Coakley and Davies (1986) who suggest that a decrease in equivalent liquid water content (EQLWC) and droplet size distribution is expected where the greatest entrainment of sub-saturated ambient air occurs.

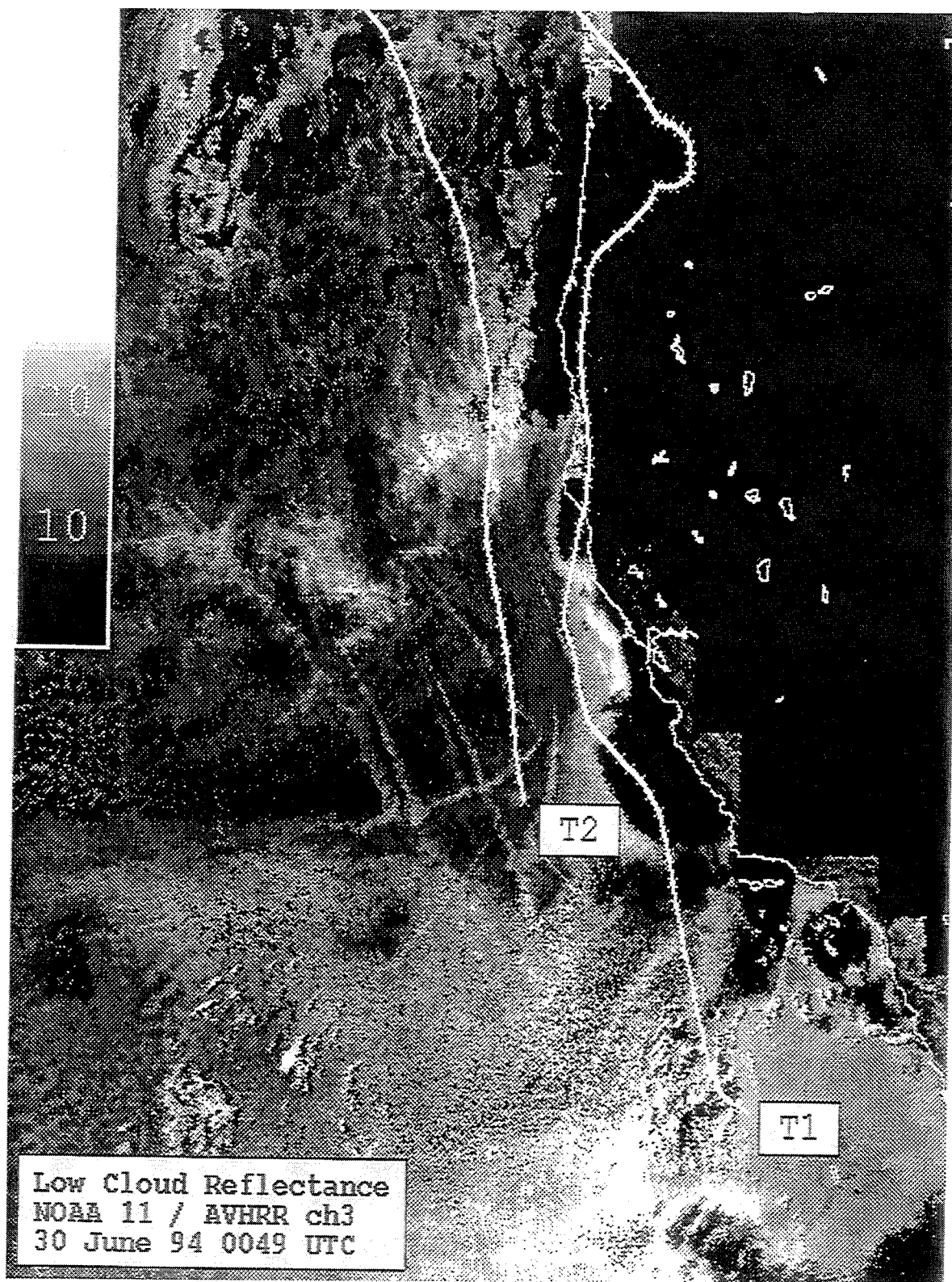


Figure 16. NOAA 11, AVHRR Channel 3 image from 30 June 1994 showing backward trajectories T1 and T2.

G. SATELLITE IMAGE COMPOSITES

Satellite image compositing techniques were utilized to illustrate the persistence of a boundary that exists between clean and dirty regions of stratus. Whenever stratocumulus clouds were observed in the region from southern California to the Baja Peninsula extending offshore, these low clouds consistently displayed increased brightness that suggests the influence of anthropogenic aerosol. Case 2 and Case 3 AVHRR channel 3 composites each contain five days of daytime passes that accentuate the persistence of this marine/continental boundary feature. Figure 17a is a composite of image passes from 13-17 June that shows the anomalous low pressure passage during Case 2. The boundary between clean and dirty stratus is located roughly along a line extending southwest from Los Angeles. This large-scale region of brightening is referred to as the "West Coast Plume" (WCP). Figure 17b represents a composite of the more typical climatology during Case 3 and contains passes from 19-23 June. The marine/continental boundary in this composite is located significantly further north and west than in Figure 17a. The difference in boundary location between the composites shows the effect of different weather on the WCP. Additionally, the composite technique demonstrates the persistence and longevity of the dirty cloud regions.

1. Comparative Streamline Analysis For 13 June and 21 June

Streamline analysis from NORAPS further illustrates the vastly different flow regimes that impact Case 2 and Case 3. As shown in Figure 18, the low-level synoptic flow on 13 June is from the north north-west, suggesting strong flow of low CCN, clean Pacific air pushing up against the California coast. The synoptic low pressure center off Vancouver Island has disturbed the more typical low-level flow, between slow moving Pacific anticyclone and persistent California thermal low, resulting in greater onshore flow along the entire west coast at the surface and 925mb. This onshore flow diverges along 140°N; coastal flow to the south pumps clean air into the operating area pushing the dirty stratus against the Baja Peninsula (Fig. 10).

Figure 19 depicts a NORAPS surface streamline analysis for 21 June. It is consistent

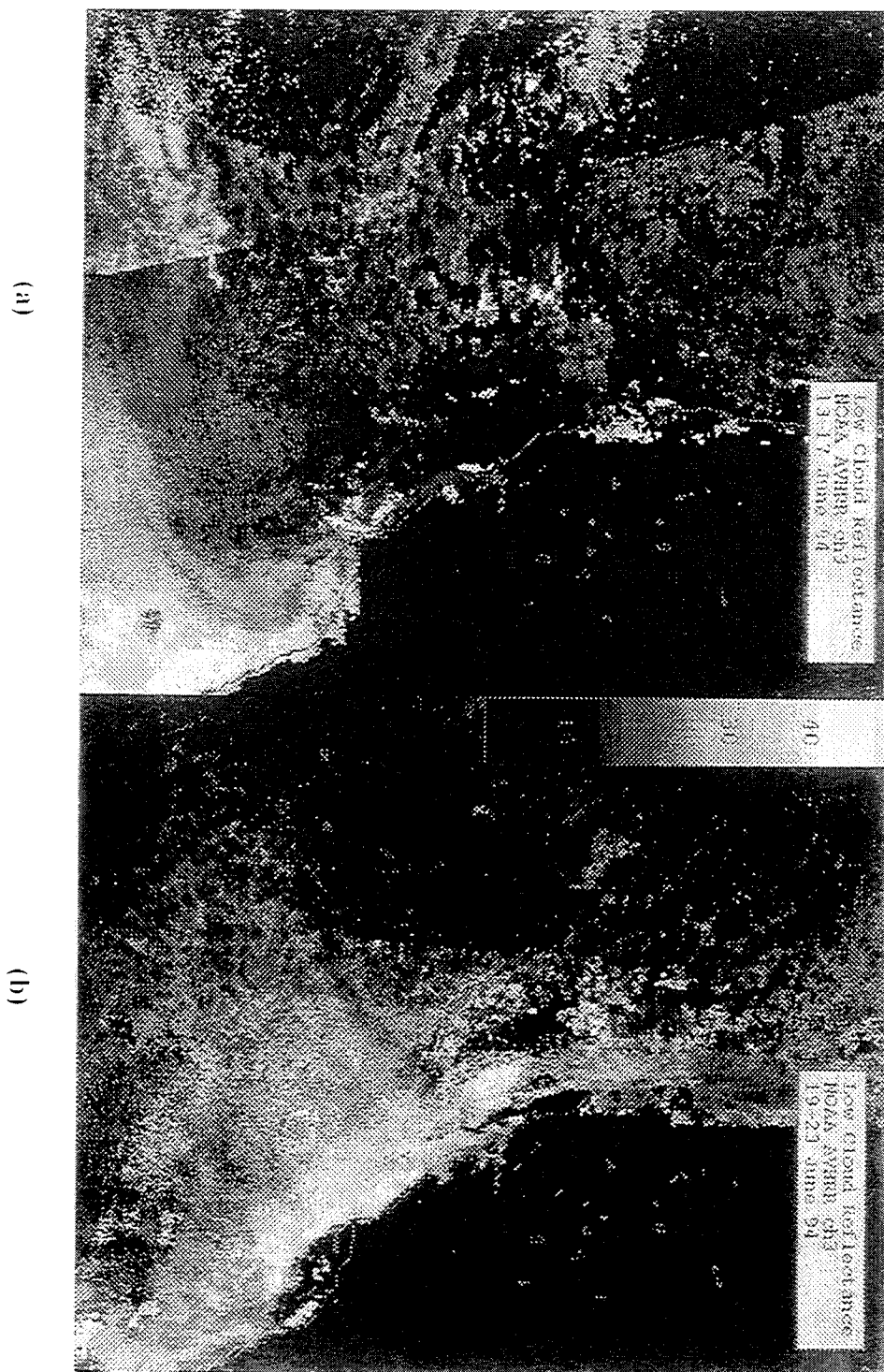
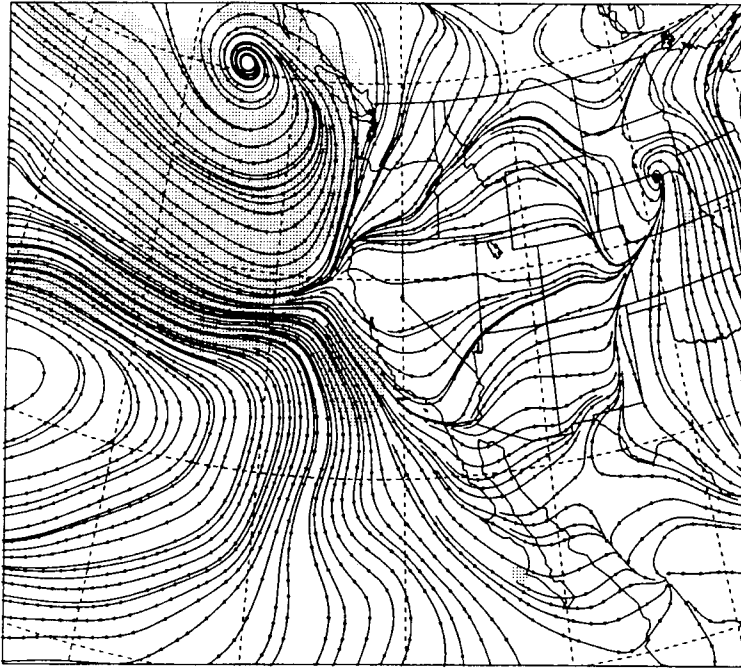


Figure 17 NOAA AVHRR Channel 3 image composites of daytime passes from (a) 13 to 17 June 1994 and (b) 19 to 23 June 1994.

sfc streamlines iso



925 mb streamlines iso

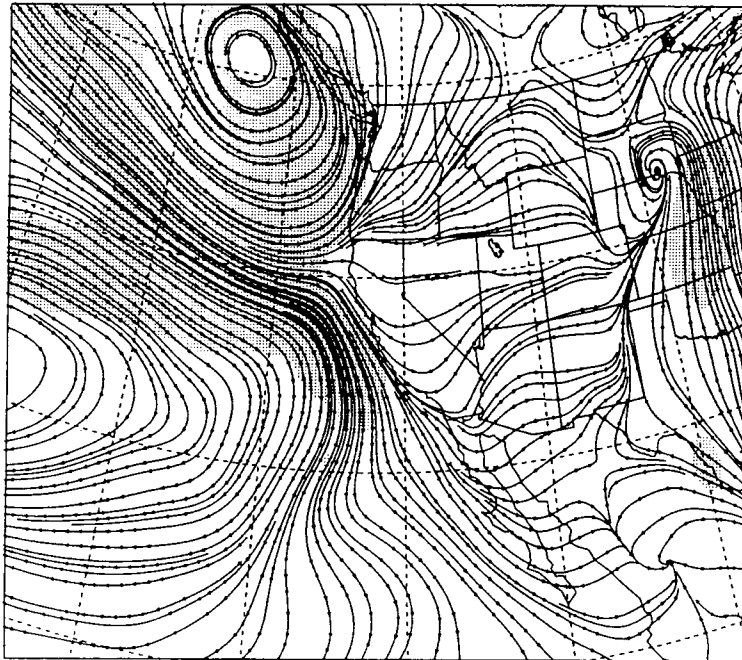
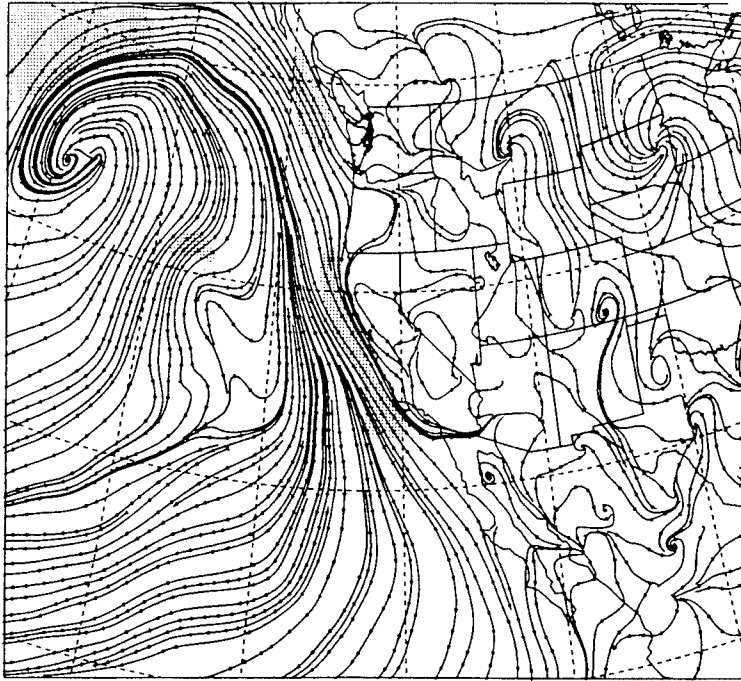


Figure 18. NORAPS Model streamline analysis 0000 UTC, 13 June 1994, showing the effect of low pressure influence at the surface and 925mb.

sfc streamlines iso



925 mb streamlines iso

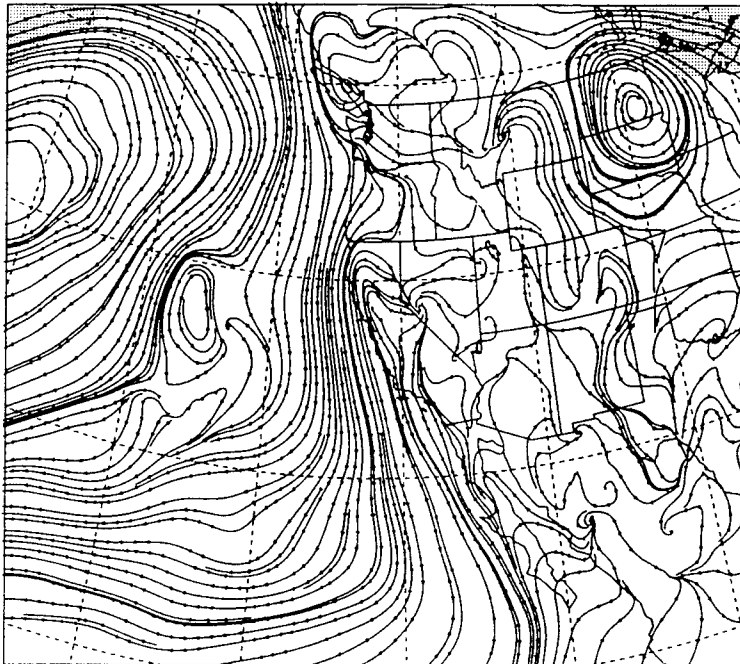
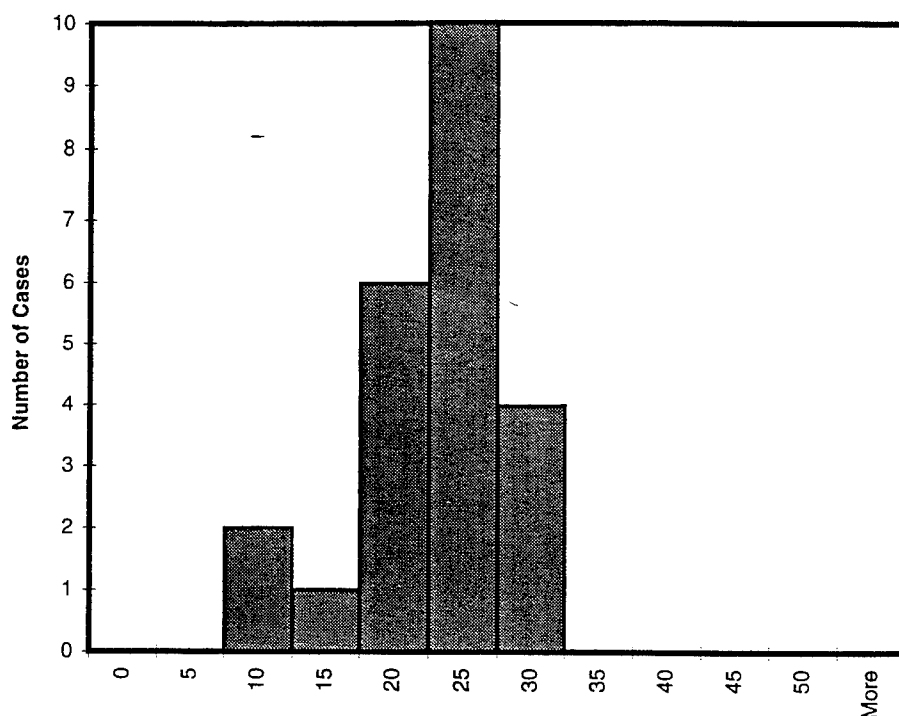


Figure 19. NORAPS Model streamline analysis 1200 UTC, 21 June 1994, depicting flow associated with typical synoptic conditions in the eastern Pacific.

with climatology and the streamlines exhibit general northerly flow along the California coast. At 925mb, there is offshore flow stretching from Oregon down to southern California. This offshore flow is consistent with Case 3, T1 and Case 3, T2 as the trajectories are collocated in bright stratus. Further comparison between these cases reveals different air mass flow at 31°N/124°W. Case 2, T2 is classified marine and consistent with the streamline divergence mentioned above. Case 3, T2 is continentally influenced and flows toward the ITCZ along the West Coast littoral zone.

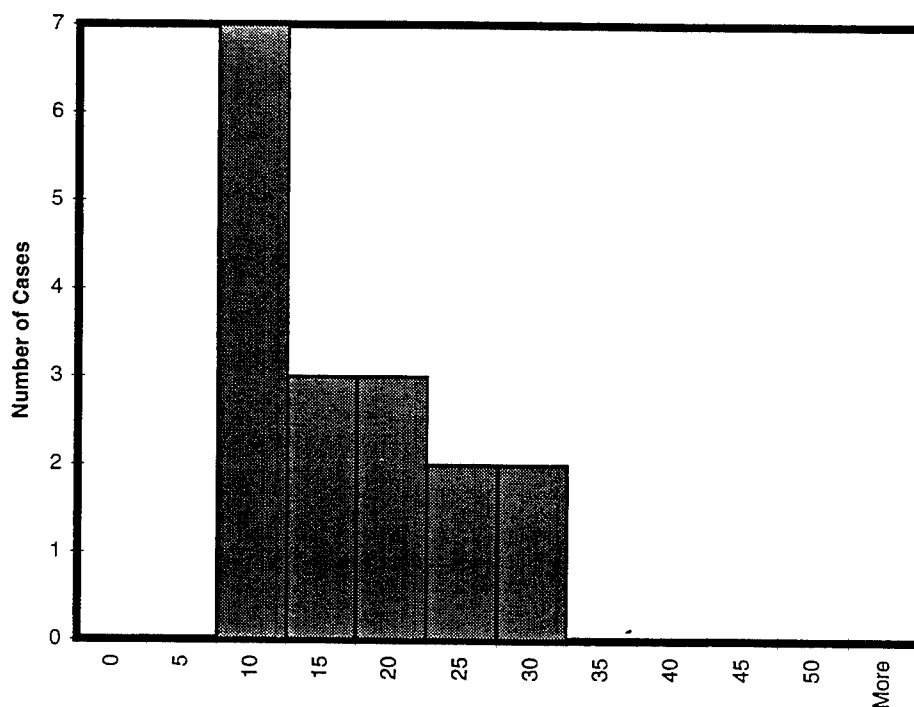
H. RESULTS

Increased numbers of aerosol result in increased cloud albedo as discussed in Chapter II. Figure 20 is a histogram of continental trajectory frequency versus channel 3 reflectance and has a mean value of 20.1 percent reflectance. In Figure 21, marine trajectories versus channel 3 reflectance are characterized by lower reflectance values of approximately 14.4 percent. AVHRR channel 3 reflectance values for the continentally influenced trajectory category versus channel 3 reflectance (Figure 22) are quite similar to continental with a mean value equal to 21.3 percent. Figure 23 is a graphical composite of all three classifications of trajectories. A t-test, assuming unequal variance, shows a probability of only 1.5 percent that the continental and marine trajectories are statistically equivalent. Therefore, with a high degree of confidence, continental trajectories in this study, produce brighter clouds than marine trajectories. The similar profile of continental and continental influenced trajectories in contrast to marine trajectories is clearly observed. The similar reflectance values of the former two trajectory types is not unexpected considering the complex interactions along a coastal environment. Continental aerosols get caught up in the sea breeze and circulated up and down the coast. Peninsulas and other complex coastal topography can increase upward motion, pulling surface aerosol sources into the boundary layer. Low level wind direction shifts due to coriolis and baroclinicity between land and sea further complicate flow regimes.



Low Cloud Reflectance at 3.7microns

Figure 20. Histogram of continental trajectory frequency versus AVHRR channel 3, low cloud reflectance at 3.7 microns.



Low Cloud Reflectance at 3.7microns

Figure 21. Histogram of marine trajectory frequency versus AVHRR channel 3, low cloud reflectance at 3.7 microns.

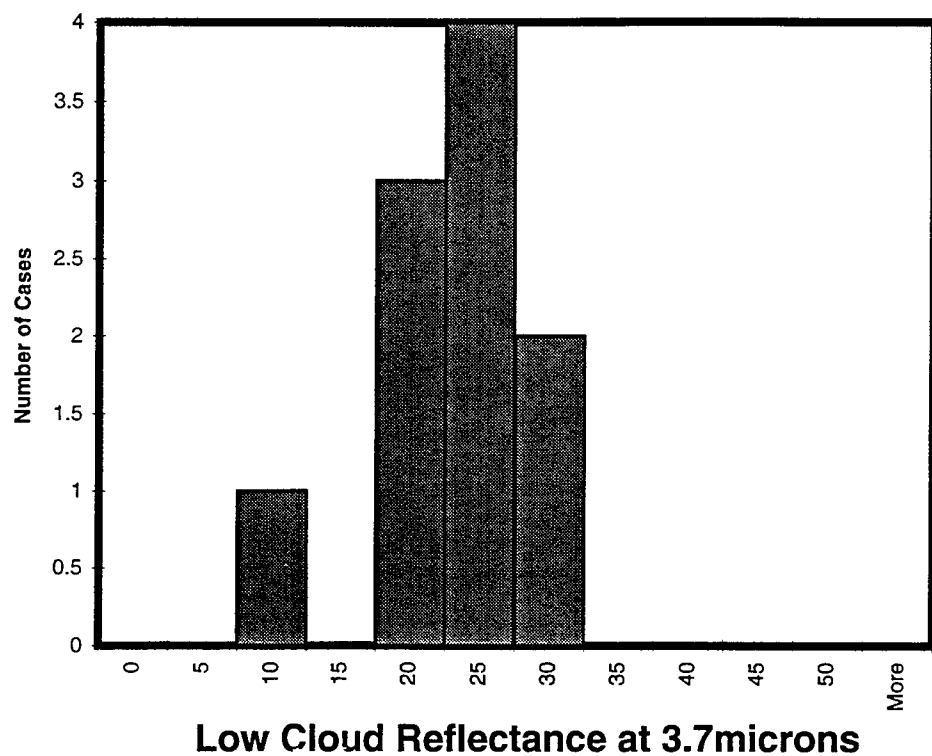


Figure 22. Histogram of continental influenced trajectory frequency versus AVHRR channel 3, low cloud reflectance at 3.7 microns.

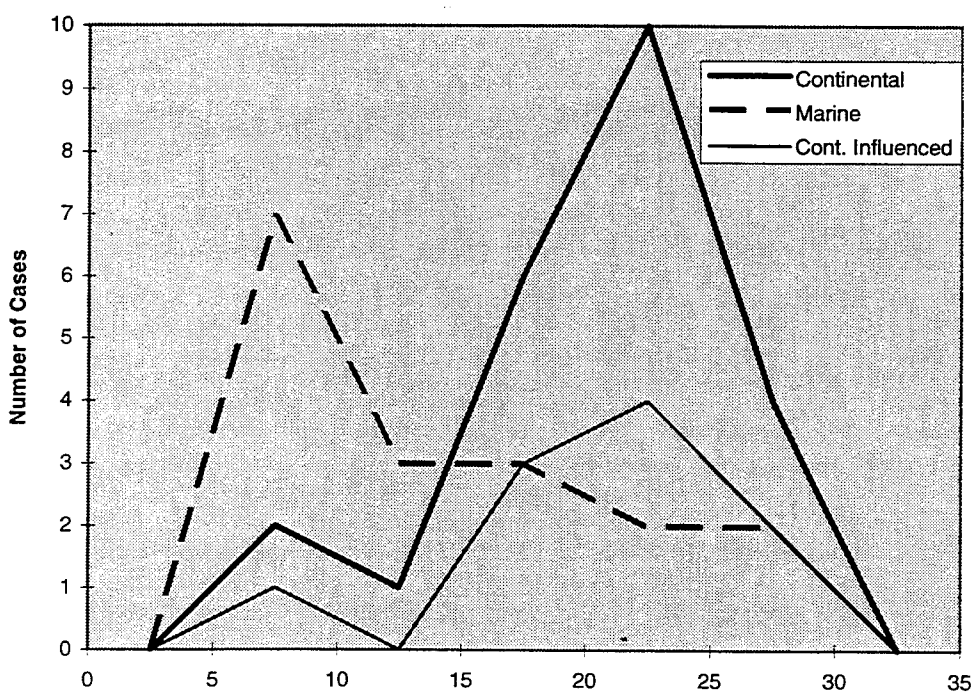


Figure 23. Graphic composite of 3 trajectory types analyzed: continental, marine and continentally influenced. Y axis is number of cases. X axis is AVHRR low cloud reflectance at 3.7 microns. Note the similarity of solid curves (continental and continentally influenced) in contrast with dashed line, marine trajectories.

V. CONCLUSIONS AND RECOMMENDATIONS

A. CONCLUSIONS

The relationship between continentally affected air masses and cloud reflectance at $3.7\ \mu\text{m}$ has been illustrated through the use of AVHRR channel 3 satellite data and NOAA's HY-SPLIT long-range trajectory model. The anticipated relationship of higher reflectance values from air influenced by offshore flow of continental aerosol is confirmed through the case studies and statistical analysis. The continental trajectories assimilated in this thesis have a mean reflectance value of 20.1 percent. The set of trajectories classified as marine, that is they exhibit no interaction with the coastal environment, produce mean reflectance values of 14.4 percent. The lower reflectance values were expected because this air is advected in from the Pacific Ocean where aerosol and CCN numbers are at reduced levels. Continental influenced trajectory reflectance values were similar to continental values. These trajectories which travel along the land-sea boundary, without actually passing over land, had a mean reflectance value of 21.3 percent.

Clouds are a key factor in atmospheric radiative processes. Increasing the sources of anthropogenic aerosols affect cloud microphysics by increasing the albedo of relatively thin maritime stratus clouds. The spatial scale examined in this study is more than a factor of ten greater than the shiptrack phenomenon, but analogous in dynamical forcing. This microphysical change in cloud albedo is considered an indirect forcing mechanism that results in climatic cooling which may be equal in strength, but opposite in sign to greenhouse warming. The difference in mean cloud albedos illustrated in this thesis is consistent with theories relating to the profound effect humans may be exerting on the environment.

In fact, the majority of MAST satellite images with stratus clouds present off of the southern California coast exhibited some degree of increased reflectivity between 120° - 125°N and 30° - 40°N . Referred to as the West Coast Plume, this region of brightening results from low-level synoptic, NW flow that does not even need to shift offshore to advect increasing amounts of particulates in the form of aerosols into the marine environment. Mesoscale sea-breeze and associated upper-level return flow, thermal gradient flow, land-

breeze flow and complex coastal topography are a few proposed mechanisms that inject anthropogenic aerosol into the coastal environment. This NW synoptic flow acts as a huge "aerosol conveyor belt," picking up greater amounts of aerosol as it flows down the coast, and eventually spills out into and around the Los Angeles Basin. Assuming no drizzle or dry deposition, continental aerosol and CCN numbers continue to increase as smaller scale processes "pile" greater amounts of dirty air onto the "belt." Considering that the aerosol laden air mass flows over one of the most fertile valleys in the world and a variety of terrain that includes densely populated urban areas (e.g., San Francisco), it is really no surprise that man's signature is clearly written in the clouds.

B. RECOMMENDATIONS

MAST aircraft data will provide an abundance of insight into the detailed microstructure of stratocumulus clouds. These in-situ measurements will offer clues to the specific types of aerosols in question for a forward trajectory analysis study. The same HY-SPLIT model and dataset could be employed in this fashion. Another back trajectory study is recommended to ascertain chemical origins of aerosols. Due to the limited scope of sampling available with aircraft filtering devices, this would best be accomplished running HY-SPLIT with a finer resolution dataset or with a different mesoscale trajectory and diffusion model.

Further observations of marine stratocumulus clouds, such as those that occur with great regularity off the west coast of the continental U. S., should be studied globally to attempt to quantify their significance. A more detailed understanding of the mechanisms that cause, and the areas that are effected by, continental aerosol would assist coastal military weapons platforms. Knowledge of the threshold of CCN numbers that inhibit shiptrack signature has obvious intelligence implications.

The single largest improvement to an experiment of this nature, and beneficial to all realms of study, would be the use of a sampling instrument with better 'on station' time. Remotely piloted unmanned drones will eventually fill this need.

APPENDIX. SYNOPTIC WEATHER SUMMARY FOR MAST (June '94)

Tools:

- NMC Surface Analysis Charts
- GOES Satellite Imagery
- NORAPS 925mb Streamlines
- MRF Flight Summary

Streamline Flow Codes:

- 1. = Oregon on = onshore l = light
 - 2. = San Fran. of = offshore m = medium
 - 3. = L.A. pa = parallel h = heavy
- (strength of flow based on gradient)

1 June: High pressure dominates eastern Pacific with ridging extending from Oregon to 25N/135W. Mostly clear with some stratus extending from San Francisco down to Big Sur and extending to the southwest.

Streamline Flow

0000z: not available

1200z: not available

2 June: Ridge weakening (1024) off Crescent City toward southwest. Front pushing in from east. Residual stratus breaking up.

Streamline Flow

0600z: 1.of/m 2.of/l 3.pa/ml

1200z: 1.of/ml 2.of/m 3.pa/ml

3 June: Continuing slow changing summer pattern with residual stratus around Bay area, thicker stratus 'pushed' up against coast in vicinity of weak low.

Streamline Flow

0000z: 1.on/l 2.pa/l 3.on/l

1200z: 1.* 2.of/m 3.of/m

* no flow

4 June: Weak ridging still extending from Oregon to 30N/135W. Weak stratus band extending from Cape Mendecino southwest off Monterey Bay.

Streamline Flow

0000z: 1.on/l 2.pa/ml 3.pa/ml

1200z: 1.on/l 2.pa/l 3.of/m

5 June: Continued weak ridging extending from San Francisco toward southwest ahead of cold front moving toward continent forcing moisture over Sierra Nevada. Active low pressure system dominant over northern Pacific. Cirrus over Sierras streaming eastward.

Streamline Flow

0000z: 1.on/l 2.on/l 3.pa/ml

1200z: 1.on/l* 2.pa/m 3.pa/ml

* southerly flow from N. Cal. northward.

6 June: Weak transitional lows extending from Oregon westward. Subtropical ridge extends from Southern California westward in behind weak frontal region. Stratus free in oparea, but lots of stratus from Baha westward.

Streamline Flow

0000z: 1.on/l 2.on/l 3.pa/ml

1200z: 1.on/l 2.pa/ml 3.of/ml

7 June: Ridge building from Oregon southwest; low to north starting to organize. No stratus off California coast, all to southwest.

Streamline Flow

0000z: n/a

1200z: n/a

8 June: Ridge building offshore extending from 35N/135W into Idaho with associated stratus. Coastal dry slot due to offshore flow from northern Ca. down to LA.. Troughing over California's central valley.

Streamline Flow

0000z: 1.pa/m 2.pa/m 3.pa/ml

1200z: 1.pa/l 2.of/m 3.of/ml

note: a/c reports aerosol layers @ 14,000ft/10,500ft and westerly flow in afternoon.

9 June: Similar synoptic flow: ridge slightly weakening/trough more pronounced over northern California. Dry slot still present off oparea, but stratus present toward southwest.

Streamline Flow

0000z: 1.pa/m 2.pa/mh 3.of/m

1200z: 1.pa/l 2.of/m 3.of/l

note: a/c reports aerosol layer below 9000ft(afternoon)

10 June: Weak ridging from Washington State southwest. Offshore flow associated with westward moving low. Trough axis shifted west allowing southerly coastal surge of stratus.

Streamline Flow

0000z: 1.of/m 2.of/h 3.pa/l

1200z: 1.of/ml 2.of/mh 3.of/l

11 June: Pacific high ridging eastward north of California. Trough shifted back over central valley and weakening. Stratocumulus socks in from northeast into oparea south of San Francisco.

Streamline Flow

0000z: n/a

1200z: n/a

note: Clean/dirty stratus transitional sharply defined region from 36N/123W to 32N/127W.

12 June: Cold front approaching Monterey Coast with ridging south of 40N. Trough over central valley has moved well inland.

Streamline Flow

0000z: 1.on/l 2.on/m 3.on/l

1200z: 1.on/l 2.of/m 3.pa/ml

13 June: Cold front pushing in further toward Monterey Coast with associated northwesterly cirrus. Ridging south of 40N moves west toward central Pacific. Extensive stratus sheets southwest of oparea.

Streamline Flow

0000z: 1.on/m 2.pa/m 3.pa/m

1200z: 1.on/l 2.pa/m 3.of/ml

note: a/c reports 'remarkably clean boundary layer' (midday)

14 June: Frontal passage cleared out oparea (possible drying, as well, due to slight offshore flow). Weak post-frontal ridging building in. Strong inversion present above convective stratocumulus to west of oparea. Weak transient troughing waves from Gulf of Alaska down through Oregon.

Streamline Flow

0000z: 1.on/m 2.pa/m 3.pa/m

1200z: 1.on/l 2.of/m 3.of/m

note: a/c notes 'distinct haze layer visible to the naked eye' at mid-levels.

15 June: Similar synoptic pattern. Lows transit through, mixing, possibly keeping subsidence from setting up status (little stratus).

Streamline Flow

0000z: n/a

1200z: n/a

16 June: Strong anticyclone over Pacific; weak trough over valley appears ideal for stratus. Stratus looks good for tracks south of San Francisco extending toward southwest. Air mass still cooler due to low passage increasing boundary layer depth.

Streamline Flow

0000z: 1.on/l 2.pa/m 3.pa/l

1200z: 1.on/m 2.of/ml 3.of/m

17 June: Similar conditions: slight building of ridge. Stratus line extending from Big Sur thinning.

Streamline Flow

0000z: 1.on/l 2.pa/m 3.pa/l

1200z: 1.pa/m 2.pa/ml 3.pa/ml

18 June: High pressure over Pacific yields northerly flow. Subsidence further offshore with associated stratus sheets (>250nm southwest of oparea).

Streamline Flow

0000z: 1.on/l 2.pa/m 3.pa/m

1200z: 1.of/m 2.of/m 3.of/m

19 June: Anticyclonic high is dominant feature -- weak ridging extends into Washington. Offshore flow around Oregon causing dry slot.

Streamline Flow

0000z: 1.pa/m 2.on/l 3.on/ml

1200z: 1.of/m 2.pa/mh 3.of/m

20 June: Similar situation with weak thermal trough over valley. Typical stratus weather: extensive sheets in and to southwest of oparea.

Streamline Flow

0000z: 1.pa/mh 2.on/l 3.on/l (h northerlies)

1200z: 1.pa/m 2.pa/m 3.of/l

note: a/c noted how close base of cumulus clouds were to stratocumulus giving a brightening effect.

21 June: High pressure dominant over Pacific. Dry slot persists over LA. due to dry slot.

Streamline Flow

0000z: 1.on/l 2.on/l 3.on/m (northerlies)

1200z: 1.of/l 2.pa/l 3.of/l

note: aerosol concentration in the boundary relatively high.

22 June: Anticyclone has imbedded fronts propagating towards coast from northwest. Offshore flow should weaken (lesser gradient). Stratus persists.

Streamline Flow

0000z: 1.pa/m 2.pa/m 3.pa/l

1200z: 1.pa/l 2.pa/ml 3.of/l

note: a/c reports cleaner BL as progressed west.

Aerosol fluxuations: lower concentrations near cloud base than at surface.

23 June: Similar conditions with northerly surface flow. Upper level trough yields southwesterly flow at upper levels.

Streamline Flow

0000z: 1.on/l 2.on/l 3.pa/l

1200z: 1.on/l 2.pa/ml 3.pa/ml

note: clear air aerosol samples taken at different altitudes(dirtiest in BL).

24 June: Ridging pushes in from west causing deformation zone between thermal low -- resulting flow more northeasterly.

Streamline Flow

0000z: 1.on/l 2.pa/mh 3.pa/m

1200z: 1.on/l 2.pa/ml 3.of/ml

25 June: More of the same with flow shifting more northerly. Weak transient low off Oregon.

Streamline Flow

0000z: 1.on/l 2.pa/mh 3.on/m

1200z: 1.on/l 2.pa/m 3.of/m

26 June: High pressure region building slightly and extending into Oregon/Idaho.

Streamline Flow

0000z: 1.on/l 2.pa/m 3.on/ml

1200z: 1.on/l 2.of/m 3.of/m

27 June: Continued ridging forces flow northeasterly. A weak upper air trough passed through overnight weakening subsidence, allowing inversion to rise, letting stratus form back in/around oparea.

Streamline Flow

0000z: 1.of/m 2.pa/m 3.pa/ml

1200z: 1.of/ml 2.pa/m 3.of/m

note: clean air mass reported around 35N/125W.

28 June: Weakened ridging, less offshore wind, more stratocumulus in and around oparea.

Streamline Flow

0000z: 1.pa/m 2.on/l 3.pa/ml

1200z: 1.of/m 2.pa/ml 3.of/m

note: Distinct brown haze layer observed at 3500ft.

Higher aerosol/droplet concentrations as a/c flea east.

29 June: Strong high pressure dominates Pacific with associated northerly flow over oparea. Weak ridging over Oregon may cause slight offshore trajectories over northern California. Extensive stratus over oparea.

Streamline Flow

0000z: n/a

1200z: n/a

note: sat. imagery shows 'dirty' clouds near coast.

30 June: Similar synoptic conditions: stratus eroding a bit late in day.

Streamline Flow

0000z: 1.pa/mh 2.pa/m 3.on/l

1200z: 1.pa/m 2.pa/m 3.of/l

LIST OF REFERENCES

- Albrecht, B. A., 1989: Aerosols, cloud microphysics, and fractional cloudiness. *Science* **245**, 1227-1230.
- Andreae, M. O., 1994: Climatic effects of changing atmospheric aerosol levels. *World Survey Clim., Future Clim. of the World*, A. Henderson-Sellers, Ed., Elsevier, in press.
- Bloembergen, N., C. K. Patel and G. Pake (chairpersons), 1987: Science and Technology of Directed Energy Weapons. Report of the American Physical Society Study Group, *Reviews of Modern Physics*, **59**, S1-S202.
- Charlson, R. J., J. Langner, H. Rodhe, C. B. Leovy, and S. G. Warren, 1991: Perturbation of the Northern Hemisphere radiative balance by backscattering from anthropogenic sulfate aerosols. *Tellus*, **43 AB**, 152-163.
- Coakley, J. A., Jr., and R. Davies, 1986: The effect of cloud sides on reflected solar radiation as deduced from satellite observations. *J. Atmos. Sci.*, **43**, 1025-1035.
- Coakley, J. A., Jr., R. L. Bernstein and P. A. Durkee, 1987: Effect of ship stack Effluents on cloud reflectivity. *Science*, **237**, 953-1084.
- Conover, J. H., 1966: Anomalous cloud lines, *J. Atmos. Sci.*, **23**, 778-785.
- Cordray, D. M., J. W. Fitzgerald, S. G. Gathman, J. N. Hayes, J. E. Kenney, G. P. Mueller and R.E. Ruskin, 1977: Meteorological Sensitivity Study on High Energy Laser Propagation. Naval Research Laboratory Report 8097, Washington, D. C., 81 pp.
- Draxler, R. R., 1982: Measuring and modeling the transport and dispersion of Kr-85 1500 km from a point source. *Atmos. Environ.*, **16**, 2763-2776.
- Draxler, R. R., and A. D. Taylor, 1982: Horizontal dispersion parameters for long-range transport modeling. *J. Appl. Met.*, **27**, 617-625.
- Draxler, R. R., 1987: Sensitivity of a trajectory model to the spatial and temporal resolution of the meteorological data during CAPTEX. *J. Clim. Appl. Met.*, **26**, 1577-1588.
- Draxler, R. R., 1992: Hybrid Single-Particle Lagrangian Integrated Trajectories (HY-SPLIT): version 3.0 - user's guide and model description. NOAA Tech. Memo. ERL ARL-195, June, National Technical Information Service, Springfield, VA, 26 pp.

- Hansen, J., A. A. Lacis, D. Rind, G. Russel, P. Stone, I. Fung, R. Ruedy, and J. Lerner, 1984: Analysis of feedback mechanismx. *Clim. Processes & Clim. Sensitivity*, J. E. Hansen and T. Takahashi, Eds., Amer. Geophys. Union, 130-163.
- Hindman, E. E., II, P. V. Hobbs and L. F. Radke, 1977: Cloud condensation nucleus size distributions and their effects on cloud droplet size distributions. *J. Atmos. Sci.*, **34**, 951-956.
- Hindman, Edward E., 1990: Reprints cloud physics conference 23-27 July, 1990, San Francisco, Ca. A.M.S.
- Hobbs, P. V., 1993: Aerosol-Cloud-Climate Interactions. Academic Press, Inc., London, 235 pp.
- Kaufman, Y. J., and T. Nakajima, 1993: Effect of Amazon smoke on cloud microphysics and albedo - analysis from satellite imagery. *J. Appl. Met.*, **32**, pp 729-744.
- King, M. D., F. R. Lawrence and P. V. Hobbs, 1993: Optical Properties of Marine Stratocumulus Clouds Modified by Ships. *J. Geophysical Research*, **98**, 2729-2739.
- Klein, S. A., and D. L. Hartmann, 1993: The seasonal cycle of low stratiform clouds. *J. Climate*, **6**, 1587-1606.
- Liou, K. N., 1980: An Introduction to Atmospheric Radiation. Academic Press, New York, 392 pp.
- Milton, A. F., and R. B. Friesen, 1987: Standard Output Data Products from the NCAR Research Aviation Facility. Bulletin No. 9, National Center for Advanced Thermal Imaging Systems: LOWTRAN Revisited. Naval Research Laboratory Report 8172, Washington, D.C., 35 pp.
- Mineart, G. M., 1988: Multispectral Satellite Analysis of Marine Stratocumulus Cloud Microphysics. M. S. thesis, Navan Postgraduate School, Monterey, CA, 138 pp.
- Parungo, F., J. F. Boatman, H. Sievering, S. Wilkison, and B. Hicks, 1993: Trends in global marine cloudiness and anthropogenic sulfur. *J. Climate*, **7**, 434-440.
- Platnick, S. E., and S. Twomey, 1994: Determining the susceptibility of cloud albedo changes in droplet concentration with the Advanced Very High Resolution Radiometer. *J. Appl. Meteor.*, **33**, 334-347.
- Porch, W. M., J. K. Chih-Yue, and R. G. Kelley, 1990: Ship trail and ship induced cloud dynamics. *Atmospheric Environment*, **24A**, 1051-1059.
- Radke, L. F., J. A. Coakley, and M. D. King, 1989: Direct and remote sensing observations of the effects of ships on clouds. *Science*, **246**, 1146-1149.

- Trehubenko, E. J., 1994: Shiptracks in the Californian Stratus Region: Dependency on Marine Atmospheric Boundary Layer Depth. M. S. thesis, Naval Postgraduate School, Monterey, CA, 87 pp.
- Twomey, S. A., Piepgrass, M., Wolfe, T. L., 1984: An assessment of the impact of pollution on the global cloud albedo. *Tellus*, **36B**, 365-366.
- Warner, J. and S. Twomey, 1967: The production of cloud nuclei by cane fires and the effect on cloud droplet concentration. *J. Atmos. Sci.*, **24**, 704-706.

INITIAL DISTRIBUTION LIST

		No. Copies
1.	Defense Technical Information Center Cameron Station Alexandria, VA 22304-6145	2
2.	Library, Code 52 Naval Postgraduate School Monterey, CA 93943-5101	2
3.	Chairman (Code MR/Hy) Department of Meteorology Naval Postgraduate School Monterey, CA 93943-5002	1
4.	Chairman (Code OC/Bf) Department of Oceanography Naval Postgraduate School Monterey, CA 93943-5002	1
5.	Professor Philip A. Durkee (Code MR/De) Department of Oceanography Naval Postgraduate School Monterey, CA 93943-5002	2
6.	Professor Wendell A. Nuss (Code MR/Nu) Department of Oceanography Naval Postgraduate School Monterey, CA 93943-5002	1
7.	Mr. Bob Bluth Code 4513 Office of Naval Research Room 522 800 North Quincy St. Arlington, VA 22217-5000	1
8.	Dr. David Johnson Code 1243 Office of Naval Research Room 522 800 North Quincy St. Arlington, VA 22217-5000	1

- | | | |
|-----|---|---|
| 9. | Oceanographer of the Navy
Naval Observatory
34th and Massachusetts Ave. NW
Washington, DC 20390-5000 | 1 |
| 10. | Commanding Officer
Naval Meteorology and Oceanography Command
Stennis Space Center, MS 39529-5000 | 1 |
| 11. | Chief of Naval Research
800 North Quincy St.
Arlington, VA 22217-5000 | 1 |
| 12. | Commanding Officer
Fleet Numerical Meteorology and Oceanography Center
Monterey, CA 93943 | 1 |
| 13. | LT Joseph R. Brenner
NAVEURMETOCCEN
PSC 819, Box 31
FPO AE 09645-3200 | 2 |